Journal of Microscopy, Vol. 200, Pt 2, November 2000, pp. 83–104.
Received 20 December 1999; accepted 16 June 2000

INVITED REVIEW

Multiphoton microscopy in life sciences

K. KÖNIG
Laser Microscopy Division, Institute of Anatomy II, Friedrich Schiller University, D-07740 Jena, Germany

Key words. Cell damage, chromosome dissection, femtosecond laser pulses, multiphoton multicolour FISH, nanosurgery, near infrared microscopy, photodynamic therapy, time-resolved microscopy, two-photon microscopy.

Summary

Near infrared (NIR) multiphoton microscopy is becoming a novel optical tool of choice for fluorescence imaging with high spatial and temporal resolution, diagnostics, photochemistry and nanoprocessing within living cells and tissues. Three-dimensional fluorescence imaging based on non-resonant two-photon or three-photon fluorophor excitation requires light intensities in the range of MW cm^{-2} to GW cm^{-2}, which can be derived by diffraction limited focusing of continuous wave and pulsed NIR laser radiation. NIR lasers can be employed as the excitation source for multifluorophor multiphoton excitation and hence multicolour imaging. In combination with fluorescence *in situ* hybridization (FISH), this novel approach can be used for multi-gene detection (multiphoton multicolour FISH). Owing to the high NIR penetration depth, non-invasive optical biopsies can be obtained from patients and *ex vivo* tissue by morphological and functional fluorescence imaging of endogenous fluorophores such as NAD(P)H, flavin, lipofuscin, porphyrins, collagen and elastin. Recent botanical applications of multiphoton microscopy include depth-resolved imaging of pigments (chlorophyll) and green fluorescent proteins as well as non-invasive fluorophore loading into single living plant cells.

Non-destructive fluorescence imaging with multiphoton microscopes is limited to an optical window. Above certain intensities, multiphoton laser microscopy leads to impaired cellular reproduction, formation of giant cells, oxidative stress and apoptosis-like cell death. Major intracellular targets of photodamage in animal cells are mitochondria as well as the Golgi apparatus. The damage is most likely based on a two-photon excitation process rather than a one-photon or three-photon event. Picosecond and femtosecond laser microscopes therefore provide approximately the same safe relative optical window for two-photon vital cell studies. In labelled cells, additional phototoxic effects may occur via photodynamic action. This has been demonstrated for aminolevulinic acid-induced protoporphyrin IX and other porphyrin sensitizers in cells. When the light intensity in NIR microscopes is increased to TW cm^{-2} levels, highly localized optical breakdown and plasma formation do occur. These femtosecond NIR laser microscopes can also be used as novel ultraprecise nanosurgical tools with cut sizes between 100 nm and 300 nm. Using the versatile nanoscalpel, intracellular dissection of chromosomes within living cells can be performed without perturbing the outer cell membrane. Moreover, cells remain alive. Non-invasive NIR laser surgery within a living cell or within an organelle is therefore possible.

1. Introduction

Conventional light microscopes used in life sciences are based on the use of ultraviolet (UV) and visible (VIS) radiation for optical analysis and microsurgery (Minsky, 1988; Greulich & Weber, 1992; Pawley, 1995). The diagnostic methods include (i) 2D fluorescence microscopy using discrete excitation lines of high pressure mercury lamps and (ii) 3D confocal laser scanning fluorescence microscopy with excitation radiation of He–Ne lasers, argon/krypton ion lasers, He–Cd lasers and laser diodes.

Most endogenous fluorophores in cells, such as tryptophan, NAD(P)H and flavins, require UV or blue excitation wavelengths. Important exogenous fluorophores, such as the DNA markers Hoechst 33342 and DAPI (4′,6-diamidino-2-phenylindole) as well as the calcium indicators Fura-2 and Indo-1 possess absorption bands in the UV only,

Correspondence to: K. König. Fax: +49 3641 938552; e-mail: kkoe@mti-n.uni-jena.de

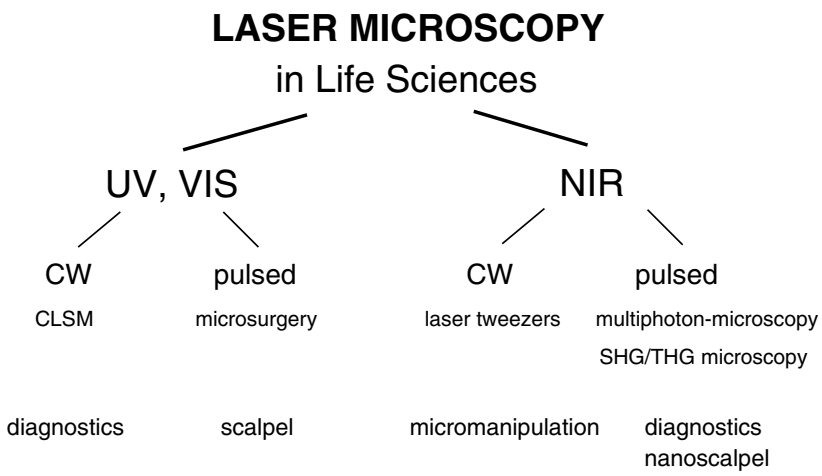

Fig. 1. Laser microscopy in life sciences. In conventional microscopy, ultraviolet and visible laser radiation are mainly used for confocal laser scanning microscopy (CLSM) and microsurgery. Major applications of NIR microscopy are optical trapping with laser tweezers and multiphoton microscopy. In addition, SHG (second harmonic generation) and THG (triple harmonic generation) microscopy have been used.

whilst other exogenous fluorophores are designed to match the laser and mercury lamp emission lines. Microsurgery of cells is typically performed with a nitrogen laser at 337 nm or the third harmonic (355 nm) and second harmonic (532 nm) of a Q-switched Nd:YAG laser (Berns, 1998; Schütze *et al.*, 1994). However, the use of UV and short-wavelength VIS radiation in conventional light microscopy has disadvantages mainly because of low light penetration depth and the potential of severe photodamage to living cells (Cunningham *et al.*, 1985; Tyrell & Keyse, 1990). It has been shown that fluorescence microscopy of single cells with the 365 nm radiation from a conventional 50 W high pressure mercury lamp results within seconds in failed cellular reproduction, modifications in intracellular redox state and DNA strand breaks (König *et al.*, 1996a).

A versatile innovation in live cell microscopy is based on the application of near infrared (NIR) radiation in the spectral range 700–1100 nm (Fig. 1). This range and the red region (600–700 nm) is referred to as the 'optical window' of cells and tissues owing to the lack of efficient endogenous absorbers in this spectral range and the subsequent high light penetration depth of the order of a few millimetres in most tissues (Fig. 2). Water, with a low absorption coefficient of ≤ 0.1 cm^{-1} (Hale & Querry, 1973), is considered to be the major absorber in cells without haemoglobin, melanin or chlorophyll. These non-pigmented cells therefore appear to be nearly transparent structures in the case of low intensity NIR radiation.

There are two major applications of NIR microscopy in life sciences. On one hand are the laser tweezers (optical traps) for optical micromanipulation, cell sorting, picoNewton force measurements (Ashkin & Dziedzik, 1987; Block *et al.*, 1989; Chu, 1991; Perkins *et al.*, 1994a,b; Veigel *et al.*, 1999), and diagnostics of motile cells (König *et al.*, 1998). Laser tweezers are based on the application of highly focused continuous wave (cw) NIR laser radiation with typical mean powers in the range 10–100 mW.

The other important application of NIR microscopy is two-photon and three-photon excitation that enables 3D fluorescence imaging and photoinduced uncaging of compounds. Two-photon excitation of electronic states, based on the simultaneous absorption of photons, was predicted in 1931 (Göppert-Meyer, 1931) and first realized with the availability of lasers in 1961 (Kaiser & Garret, 1961). They detected the blue fluorescence of $CaF_2 : Eu^{2+}$ crystals using red 0.5 ms pulses of a ruby laser. However, the first two-photon excited fluorescence imaging of living specimens using a 100 fs NIR dye laser was published almost 30 years later (Denk *et al.*, 1990). These authors focused the radiation to a diffraction-limited spot using a high-numerical-aperture objective of a laser scanning microscope. Today, tuneable mode-locked Ti : sapphire lasers operating at 70–80 MHz repetition rate and a pulse

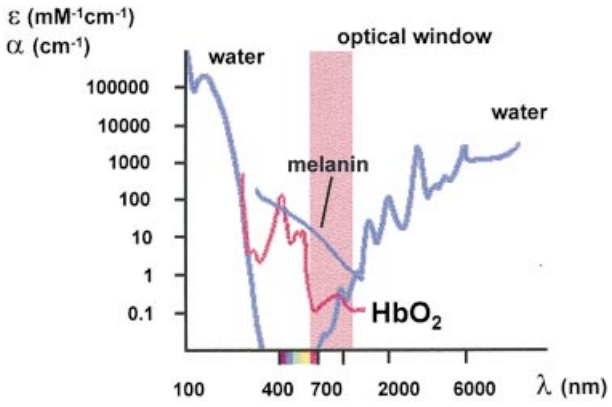

Fig. 2. Absorption spectra of major intracellular absorbers. The molecular exctinction coefficients of oxygenated haemoglobin and melanin and the absorption coefficient of water are shown. Most animal cells and tissues are considered to be nearly transparent in the spectral range from about 700 nm to 1100 nm owing to the lack of efficient one-photon absorbers.

width of less than 150 fs are typically used as NIR sources in multiphoton microscopy. Compact turn-key solid-state Ti : sapphire lasers, Cr : LiSaF or frequency-doubled fibre lasers are potentially appropriate light sources in multiphoton microscopes. Such microscopes recently became commercially available from leading suppliers of laser scanning microscopes.

This review of multiphoton microscopy focuses on recent applications in life sciences including (i) multiphoton multicolour fluorescence *in situ* hybridization (FISH), (ii) noninvasive optical biopsy, (iii) two-photon photodynamic therapy (PDT), (iv) in plant biology, (v) nanosurgery as well as (vi) studies directed towards understanding the mechanisms of cellular response to high intensity NIR radiation.

2. Experimental set-up and features of multiphoton microscopes

The major application of multiphoton microscopes in life sciences involves the excitation of routinely used intracellular fluorescent probes by the simultaneous absorption of two NIR photons (Fig. 3) or three NIR photons. Typically, the fluorophore has no one-photon absorption band in the NIR. Owing to the relatively low two-photon and three-photon absorption cross-sections of intracellular absorbers of about 10^{-48} to 10^{-50} cm^4 s photon^{-1} and 10^{-75} to 10^{-84} cm^6 (s photon^{-1})^2 (Xu *et al.*, 1995; Xu & Webb, 1996; Maiti *et al.*, 1997; Xu & Webb, 1997), respectively, non-resonant multiphoton excitation requires photon flux densities of $> 10^{24}$ photons cm^{-2} s^{-1}. Using NIR radiation in the spectral range of 700–1100 nm, light intensities in the MW cm^{-2} to GW cm^{-2} range are required. These intensities can be obtained by diffraction limited focusing cw (Hänninen *et al.*, 1994; König *et al.*, 1995) and pulsed NIR laser radiation (Denk *et al.*, 1990) of 100 mW mean power or less.

Using cw single-frequency and multifrequency NIR lasers with 100 mW power at the sample and a high numerical aperture objective, we have demonstrated two-photon excited fluorescence within a living cell (König *et al.*, 1995, 1996b; König, 1997). Fluorescence occurred only in a sub-femtolitre focal volume at MW cm^{-2} light intensities. Laser tweezers, which are based on the use of cw NIR lasers, are therefore potential sources of two-photon excitation. Using 800 nm or 1064 nm laser tweezers, cells labelled with exogenous fluorophores remained alive over extended periods of optical trapping. This is consistent with the observations that despite high light intensities in the optical trap, the temperature increase is less than 2 K, thus excluding thermal toxic effects (Liu *et al.*, 1995; Schönle & Hell *et al.*, 1998).

By means of cw lasers (Ti : sapphire laser, krypton ion laser) and scanning units, Hell's group has performed two-photon fluorescence imaging (Hänninen *et al.*, 1994; Booth & Hell, 1998). Two-photon excitation can also be realized with compact and less expensive cw laser diodes (Hänninen *et al.*, 1995; Gu & Day, 1999).

The efficiency of two-photon excitation follows a power squared relation. However, trapping effects and photothermal effects limit the use of high power cw sources for fast fluorescence scanning microscopy. Much more efficient in fast multiphoton fluorescence imaging is the use of high repetition pulsed laser systems with moderate peak power in the watt and kilowatt range but with a low mean power.

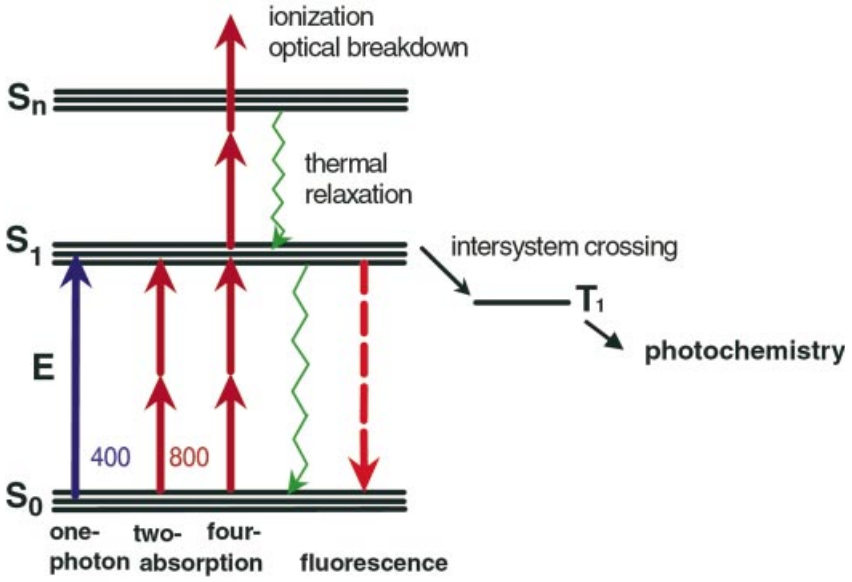

Fig. 3. Principle of non-resonant multiphoton excitation. The simultaneous absorption of two photons at MW cm^{-2} and GW cm^{-2} intensities is used in nonlinear fluorescence microscopy. At TW cm^{-2} intensities, multiphoton effects with four or more photons result in optical breakdown.

The efficiency of two-photon excitation and the fluorescence yield follows the following relation (Denk *et al.*, 1990):

$$n \approx P^2\alpha/(\tau f^2).\pi^2 \mathrm{NA}^4/(hc\lambda)^2$$

with n = number of absorbed photon pairs, P = mean power, α = molecular two-photon absorption coefficient, τ = pulse width, f = repetition frequency, NA = numerical aperture, λ = wavelength.

Because the fluorescence yield depends on a P^2/τ relation in two-photon microscopy, the efficiency increases for high peak power and low pulse width. This implies that in two-photon microscopy with 1 ps laser pulses, a mean power only three times higher is required compared to 110 fs pulses in order to acquire the same fluorescence images.

In two-photon laser microscopy the use of extremely ultrashort laser pulses (< 50 fs) at the sample has several disadvantages: substantial technical efforts are required to achieve an *in situ* pulse width (pulse width at the sample) of less than 100 fs because of the pulse broadening during transmission through the whole optical system due to optical dispersion. The major impact is from the objective, which may consist of a variety of different glass types and thicknesses. Typical optical dispersion values D for glasses in objectives at 800 nm are + 251 fs^2 cm^{-1} for CaF_2, + 300 fs^2 cm^{-1} for quartz, + 389 fs^2 cm^{-1} for FK-3, + 445 fs^2 cm^{-1} for BK7 glass, + 1030 fs^2 cm^{-1} for SF2, and + 1600 fs^2 cm^{-1} for SF10. At shorter wavelengths, these numbers increase.

In the case of chirp-free entrance pulses with a pulse width τ_{in}, the pulse broadening B can be calculated as follows:

$$B = \tau_{out}/\tau_{in} = (1 + 7.68S^2)^{0.5}$$

with $S = DL/\tau_{in}^2$. A typical DL value of the whole microscope at 800 nm including high NA oil objective is 5000 fs^2 (König, 1999). Figure 4 shows the pulse broadening in the case of an assumed 'CaF_2 objective' (DL = 930 fs^2) and of a realistic microscope system with DL = 5450 fs^2. A chirp-free laser pulse width, e.g. 10 fs will result in an *in situ* pulse width of more than 1 ps. In order to obtain *in situ* pulse widths less than 100 fs, pulse compression units consisting of optical elements of negative dispersion values (Soeller & Cannell, 1996; König, 1999) or laser systems with negative chirp output are required. Very short laser pulses experience the additional problem of large spectral bandwidth (10 fs pulses have about 100 nm bandwidth), which requires efforts to realize transmission without chromatic aberration. As shown in section 8, ultrashort pulses are more destructive than longer pulses at same pulse energy. With a typical laser pulse width of commercially available femtosecond lasers of 50–200 fs, the *in situ* pulse width is of the order of 150–250 fs. This pulse width is widely used in two-photon fluorescence microscopy (König *et al.*, 1996d). In addition, two-photon 'picosecond' systems are commercially available with typical pulse widths of 1–10 ps.

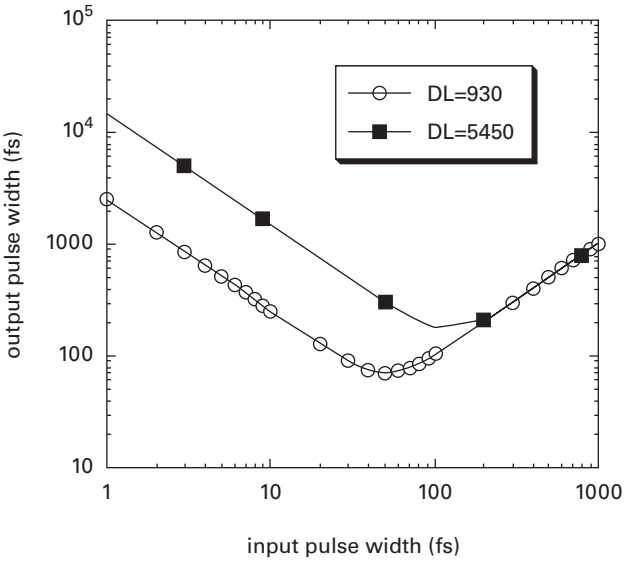

Fig. 4. Pulse broadening in CaF_2 optics (d = 32 mm) and in the optical system of a microscope including cell chamber.

Figure 5 shows our experimental set-up that routinely uses the compact solid-state femtosecond laser 'Vitesse' (Coherent, Santa Clara, U.S.A.) with 80 MHz repetition frequency, a laser wavelength of 800 nm, an output power of 1 W, and a laser pulse width of 80 fs. This laser system is easy to operate ('turn-key system') and requires no extensive water supply for cooling and no high-power supply. After expanding the NIR laser beam by a 1 : 3 Galilean telescope and the transmission through two-piece neutral density attenuators, the beam is coupled into a modified inverted confocal laser scanning microscope (LSM 410, Carl Zeiss Jena GmbH, Jena, Germany) which also incorporates a 633-nm HeNe laser for conventional CLSM. A highly reproducible mirror slider enables switching within 1 s between the visible laser and the NIR laser. The beam is focused to a diffraction-limited spot by conventional high-NA objectives onto the sample. The typical NIR transmission of the objective is 50%. When studying living cells, a closed microchamber with 170 μm thick glass windows was used ('MiniCeM', JenLab GmbH, Jena, Germany).

The microscope contains one detector for NIR transmission (brightfield, phase, differential interference contrast (DIC)) microscopy, two photomultipliers (PMTs) in the descanned mode with adjustable pinholes (spatial filters) and SP 750 short pass filters in front, and a range of detectors at the baseport. The use of a baseport detector has the advantage of detecting photons with high efficiency without transmission through the scanner and pinhole

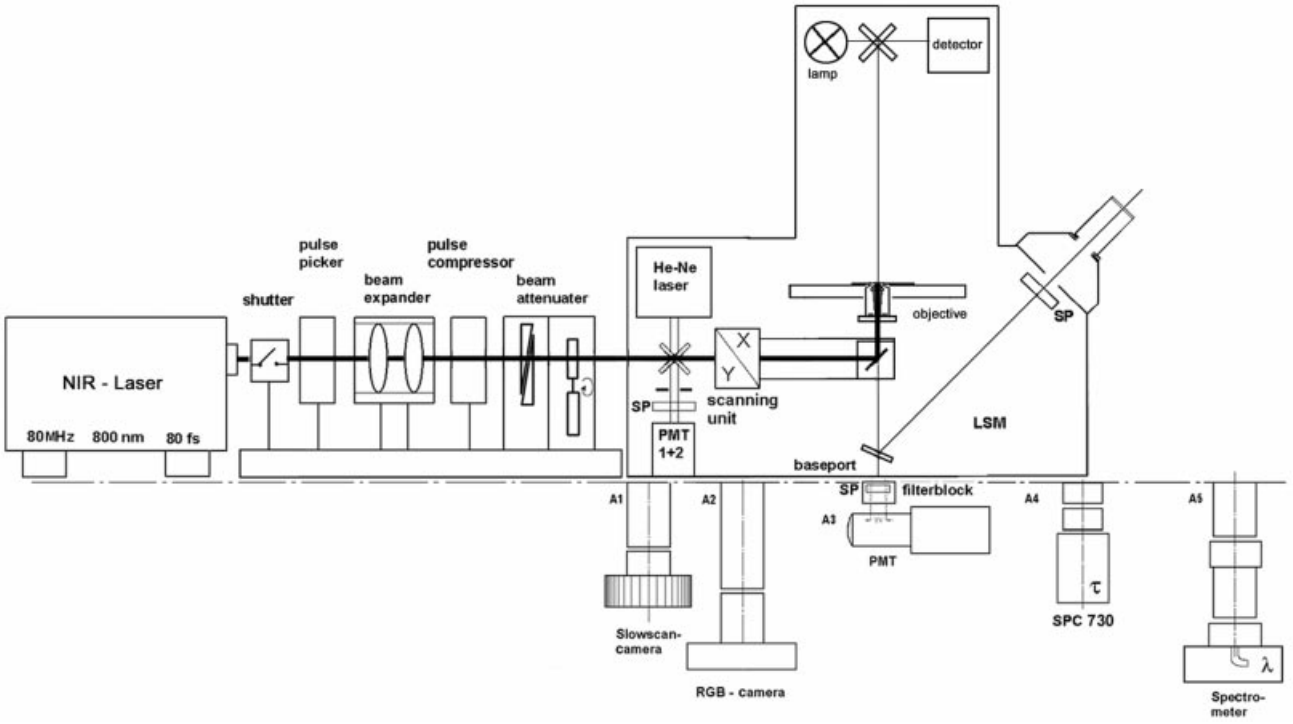

Fig. 5. Set-up of a multiphoton and one-photon confocal microscope with compact femtosecond laser source. Various detectors allow sensitive 3D black and white imaging and true colour imaging as well as spatially resolved microspectrofluorometry and τ-mapping. In addition, nanosurgery can be performed.

units. At the baseport, we use different types of PMT and cameras (e.g. colour camera, video camera, slow scan camera), an optical multichannel analyser for spectroscopy, and a single photon counting unit for time-resolved measurements. Time-resolved fluorescence measurements and spectroscopy are typically performed by scanning a region of interest (ROI) or by single point exposure, where the beam is parked at pixels of interest. The high sensitivity of the baseport PMT enables the detection of two-photon excited intracellular fluorophores with high fluorescence quantum yield (e.g. DAPI, Hoechst, Rhodamine) with a mean power at the sample of 100 μW to 1 mW at a frame rate of 1 Hz (512 × 512 pixels) (Fig. 6). More importantly, endogenous fluorophores, such as fluorescent coenzymes, can be excited with a mean power of less than 2 mW. When the power exceeds 10 mW we have detected significant cell damage. Mean powers of about 30–50 mW and μs beam dwell times per pixel are able to induce optical breakdown, which can be used to drill holes and to utilize the set-up as laser scissors, as demonstrated in section 9.

Because < 10 mW are sufficient for two-photon fluorescence excitation, only 1% of the 1 W laser output power is finally used. Instead of wasting most of the laser output, Hell's group (Bewersdorf *et al.*, 1998; Straub & Hell, 1998) suggested splitting the laser beam into beamlets using a microlens array. This multi-beam system enables an enhanced frame rate of 25 Hz (real time) or faster. It should be mentioned that the current maximum frame rate with our commercially available galvanometer scanning mirrors is 3 Hz for 512 × 512 pixels but can eventually be enhanced up to nearly 25 Hz by defining a small ROI. New developments focus on fast resonator scanners (Fan *et al.*, 1999).

The spatial resolution in two-photon fluorescence microscopy is similar to one-photon CLSM despite doubling the excitation wavelength with typical values of 0.3 μm FWHM in lateral and 0.9 μm FWHM in axial direction (Denk *et al.*, 1995). According to Stelzer *et al.* (1994), the axial resolution can be enhanced by up to 50% by the additional use of a confocal pinhole. Sako *et al.* (1997) have compared a UV-CLSM vs. two-photon microscope using the fluorophore Indo-1 and found a slightly better resolution when using a pinhole. A comparison of point spread functions in one-photon, two-photon and three-photon microscopy can be found in Schrader *et al.* (1997). Using 4 Pi two-photon microscopy, axial resolutions of about 100 nm have been demonstrated (Hell & Stelzer, 1992; Hell *et al.*, 1997; Schrader *et al.*, 1998a,b). Recently, elegant high-resolution two-photon near-field scanning microscopy has been realized (Hell *et al.*, 1998; Kirsch *et al.*, 1998; Jenei *et al.*, 1999). Furthermore, single molecule detection with two-photon fluorescence correlation

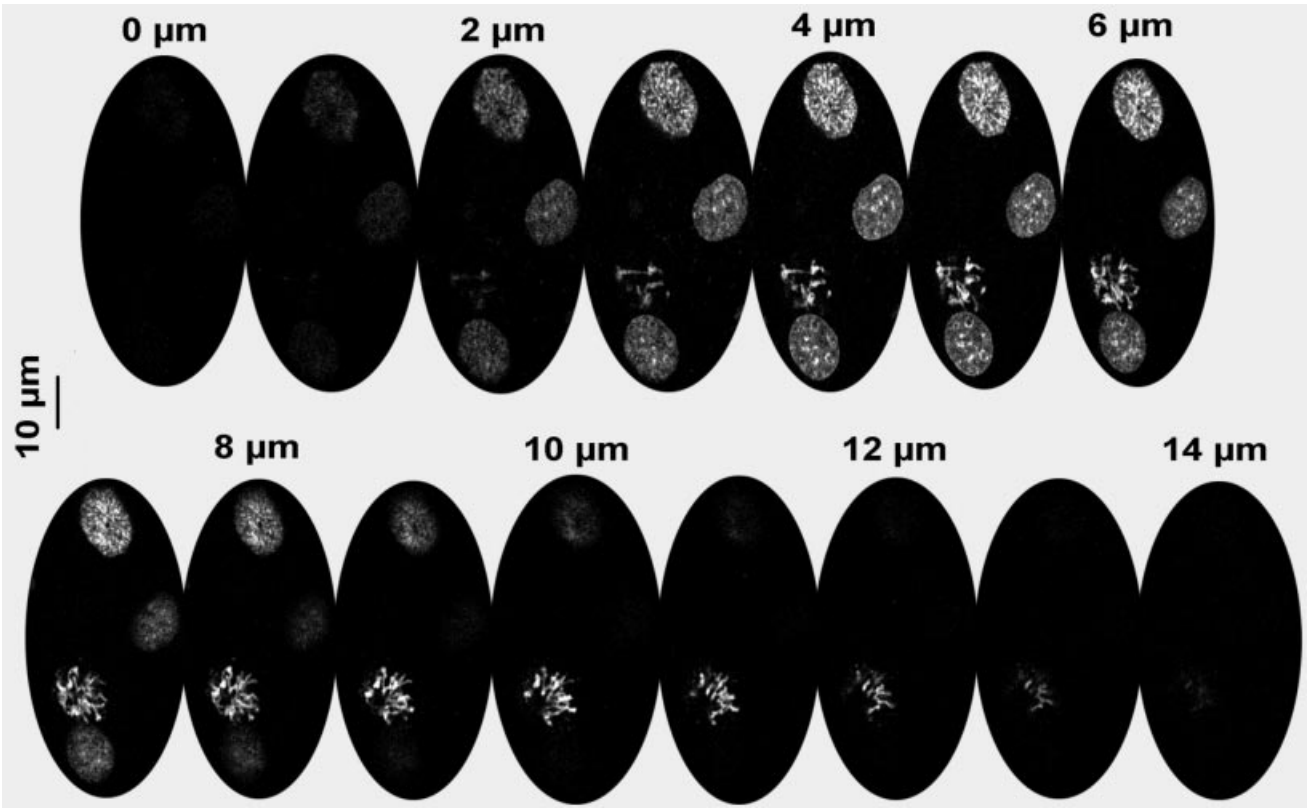

Fig. 6. 3D imaging of Hoechst 33342 in cells (right) with 170 fs pulses. Mean powers in the range 100 µW to 3 mW and µs beam dwell times per pixel are sufficient to obtain 3D fluorescence images.

spectroscopy has been demonstrated (So *et al.*, 1998; Schwille *et al.*, 1999).

3. Fluorescence lifetime measurements

Imaging of fluorescence lifetimes (τ-mapping) is a useful contrast enhancing method that provides information related to the microenvironment with spatial resolution. Different cellular probes with similar emission spectra but with different lifetimes can be distinguished. The influence of different metabolites or other environmental conditions can be studied independent of the fluorophor concentration.

The most expensive item in time-resolved microscopy with sub-nanosecond time resolution is the laser source. A femtosecond laser microscope for 3D multiphoton fluorescence imaging can be expanded to perform 3D τ-mapping.

Fluorescence lifetime imaging of living cells with femtosecond laser microscopes has been performed in the frequency domain (So *et al.*, 1995; König *et al.*, 1996c) as well as in the time domain. Time-resolved measurements in the frequency domain are based on the determination of demodulation M and phase shift ϕ and require modulated light sources (modulation frequency ω). In the case of fluorescence with monoexponential decay the lifetime τ can be deduced from the relation:

$$\omega\tau = \tan\phi = (1/M^2 - 1)^{0.5}$$

In the case of multiexponential decay, τ calculated from this relation represents the mean lifetime. The relation implies that the modulation frequency should be in the MHz range for typical ns lifetimes. The repetition frequency f of the mode-locked Ti : sapphire lasers fits the required range. In order to translate the phase and demodulation information from the 80 MHz frequency to a lower kHz frequency $d\omega$, a gain modulated detector at $(\omega + d\omega)$ frequency can be used (heterodyne technique) (So *et al.*, 1995). Low pass filtering isolates the cross-correlation signal with $d\omega$ frequency containing the same phase and demodulation as of the fluorescence signal. Figure 7 demonstrates false-colour coded lifetime imaging of the autofluorescence of Chinese hamster ovary (CHO) cells. The colours in the lifetime image represent mean lifetimes from 0 to 5 ns. Fluorescence arises mainly from mitochondria. An average lifetime of 2.2 ns was calculated from all τ-values of fluorescent 'pixels'. This lifetime value is typical for the coenzyme β-nicotinamide adenine dinucleotide (NADH) during binding to proteins (König *et al.*, 1996c).

An example of lifetime measurements in the time domain

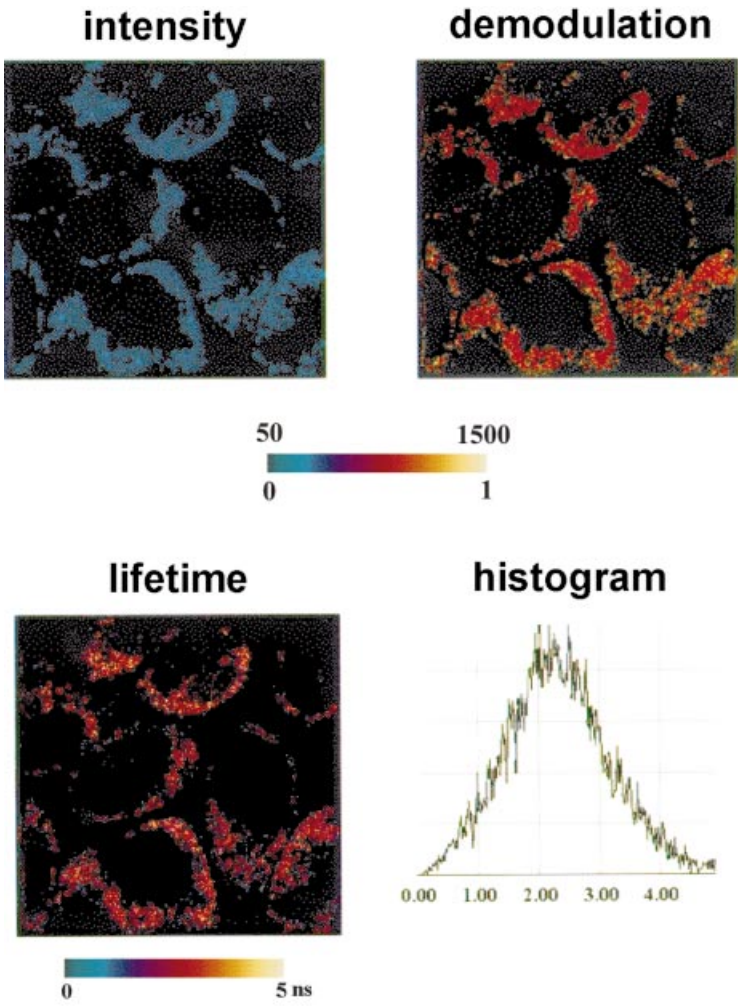

Fig. 7. Two-photon excited autofluorescence intensity image, demodulation image and mean fluorescence lifetime image and lifetime histogram of living CHO cells obtained in the frequency domain. The mean lifetime was deduced from demodulation and phase shift data.

is shown in Fig. 8. Depicted in Fig. 8, left, are fluorescence decay curves of particular regions of fluorophore-labelled cells. The information on decay kinetics was obtained by parking the laser beam ('spot mode') in pixel of interest or by line scanning and time-correlated single photon counting (SPC 730, Becker & Hickel GmbH, Berlin, Germany. In addition to single pixel fluorescence kinetics, τ-mapping was performed. The SPC unit with a channel resolution down to 800 fs allows the fast uptake and storage of $128 \times 128 = 16384$ decay curves at scanning frequency. We performed spatially resolved mapping of fluorescence decay curves (4D microscopy) of intracellular Hoechst 33342 in CHO cells with a typical frame rate of 0.1–0.02 Hz (Fig. 8, right). Furthermore, time-resolved *in vivo* autofluorescence of chlorophyll in plastids of *Arabidopsis* during division was detected (Tirlapur & König, recent unpublished results).

An alternative to the measurement of fluorescence decay curves with SPC units and subsequent calculation of a mean lifetime per pixel is time-gated fluorescence imaging using special image intensifying cameras. These cameras enable imaging at different picosecond and nanosecond time windows at a preselected time delay between excitation and detection. The cameras can be triggered at high frequencies such as 80 MHz (Straub & Hell, 1998).

4. Multiphoton multicolour FISH

An interesting feature of multiphoton NIR microscopy is multifluorophore excitation, where NIR radiation at one fixed wavelength induces simultaneously the visible fluorescence of a wide range of fluorophores with a broad multiphoton excitation spectrum. This method can be used for multicolour gene and chromosome detection, where a variety of spectrally distinct fluorescent dyes are used to label various specific regions of DNA by FISH.

FISH has emerged as an important technique in genomics for the detection of genes and chromosome regions. One of the important advantages of FISH is the possibility of detecting multiple fluorescent targets with different

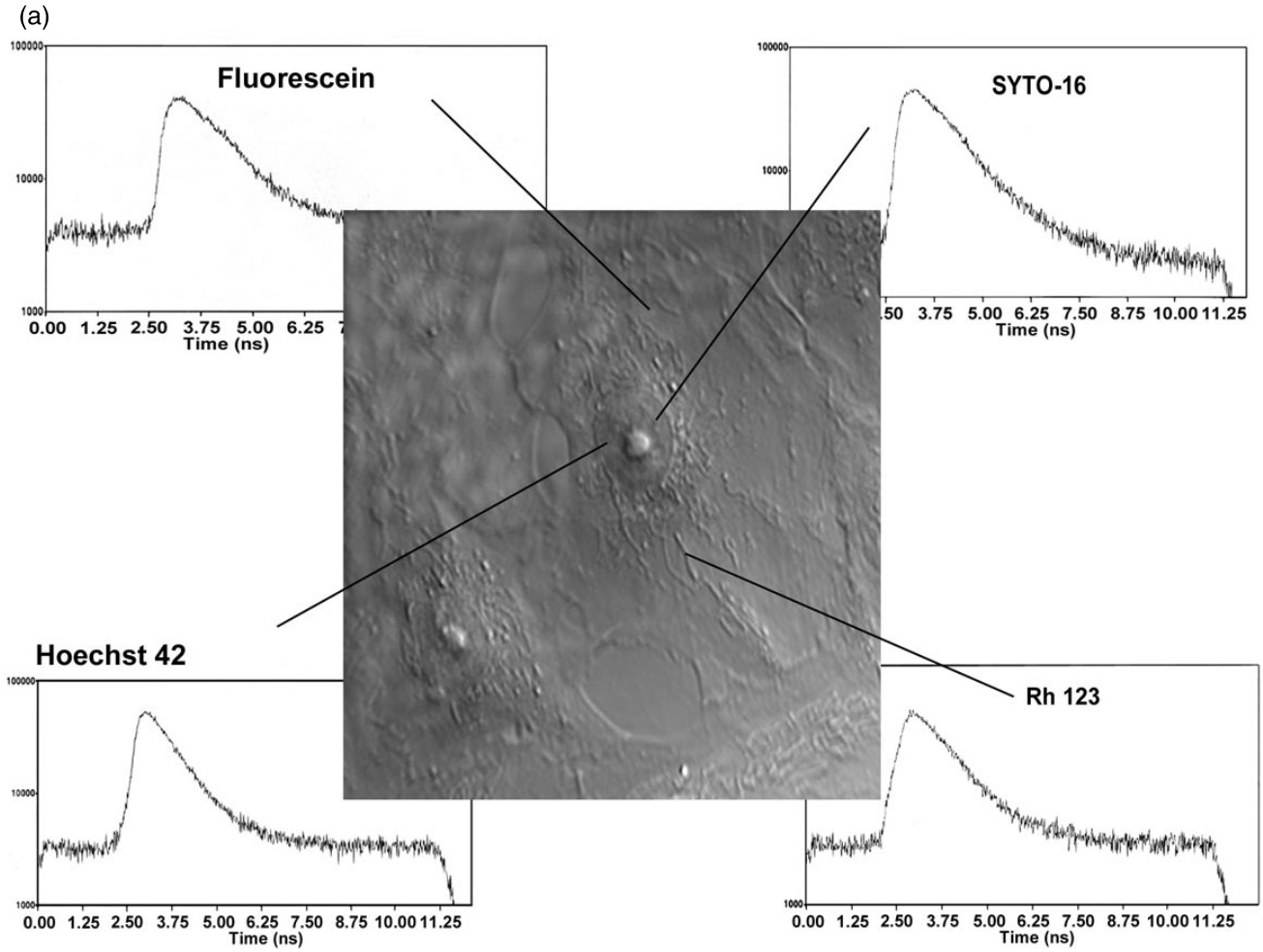

Fig. 8. (a) Fluorescence decay kinetics of 800 nm-excited fluorophores within a subcellular subfemtolitre excitation volume. The fluorophore-labelled living cell was first imaged with DIC microscopy (800 nm, 1 μW). Afterwards, the beam was parked in the subcellular area of interest and the time-resolved fluorescence was measured by single-point or line scan exposure and time-correlated single photon counting (time domain). (b) Fluorescence lifetime image of Hoechst 33342 labelled nuclei of CHO cells.

emission wavelengths for multi-gene detection (Nederlof *et al.*, 1989; Ried *et al.*, 1992; Schröck *et al.*, 1996; Speicher *et al.*, 1996; Mackville *et al.*, 1997). Until recently, different excitation wavelengths in the UV, blue and green range have been adopted to induce the visible fluorescence of the most common FISH fluorophores and of the general DNA stains such as DAPI and Hoechst 33342. However, the use of different excitation wavelengths causes problems through different wavelength-dependent focal points (chromatic aberration), the use of expensive UV optics, the separation of fluorescence and excitation photons in the case of simultaneous excitation (overlap of excitation bands and emission bands) and the beam alignment in the case of excitation with a filter wheel. These problems can be circumvented when a single NIR excitation wavelength for multicolour FISH is used. Applying radiation at 800 nm, simultaneous two-photon excitation of the blue-emitting FISH fluorophores Spectrum Aqua and Spectrum Blue (Vysis Corp., Downers Grove, U.S.A.), the green-emitting FISH fluorophores Spectrum Green (Vysis Corp.), FITC (Boehringer, Mannheim, Germany), Cy3 (Oncor, Illkrich, France), and SYBR Green (Molecular Probes, Eugene, U.S.A.) as well as the yellow/red-emitting fluorophores Rhodamine 110 (PE Applied Biosystems Inc. Forster City, U.S.A.), Spectrum Orange, Texas Red (Molecular Probes), JenFluor (JenLab GmbH), Cy 5 and Cy 5.5 (Oncor) has been realized (Fig. 9a,b). The same NIR wavelength could be used to induce the fluorescence of the general DNA/chromosome stains Hoechst, DAPI, propidium iodide and ethidium homodimer. Interestingly, the DNA stain Giemsa, which is commonly used in transmission microscopy for chromosome analysis, exhibits fluorescence when excited with intense NIR radiation. (Fig. 9c) (König *et al.*, 2000).

A further advantage of multiphoton multicolour FISH is

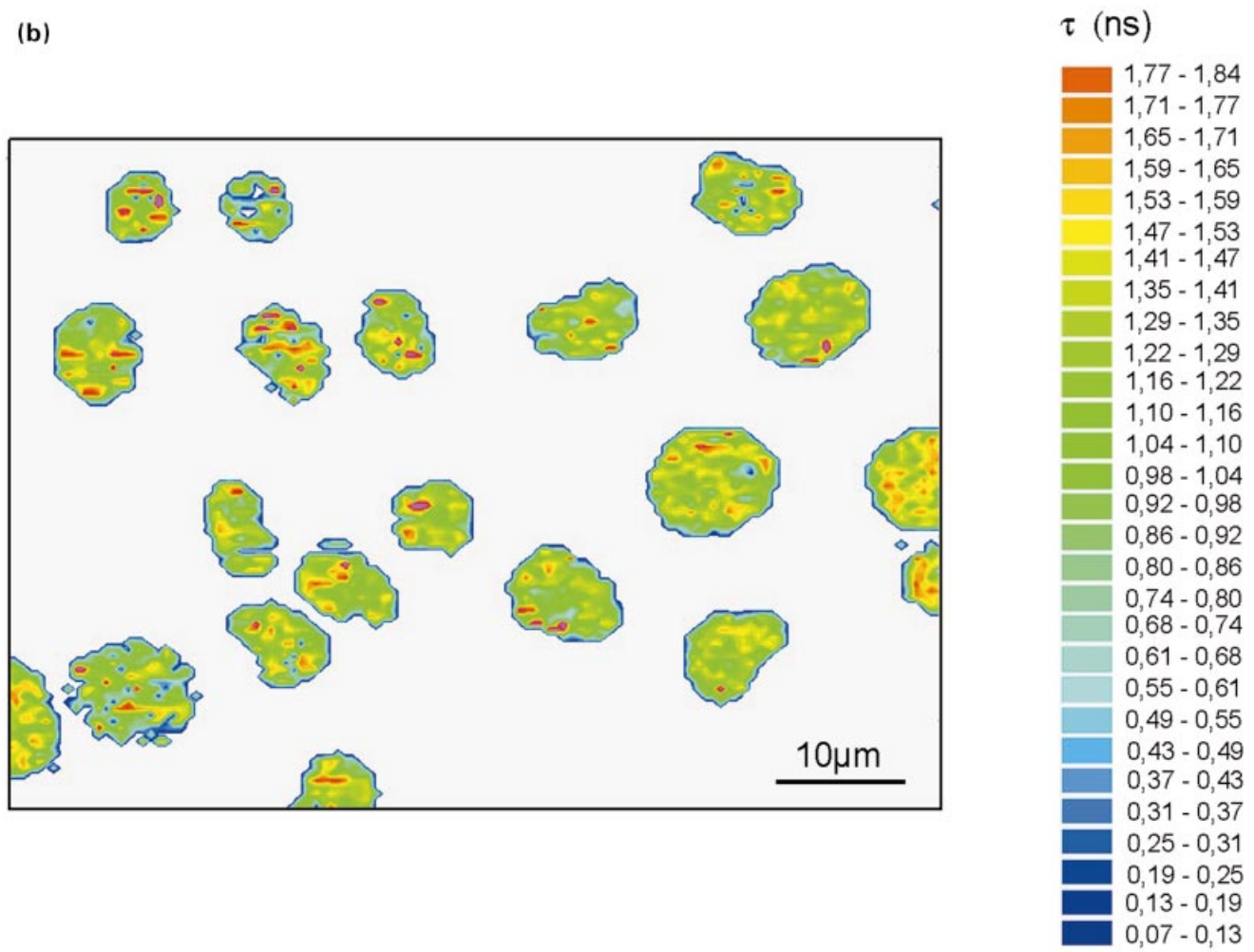

Fig. 8. Continued

the intrinsic possibility of three-dimensional fluorescence imaging. Optical sectioning allows the analysis of the architecture of the human genome. Figure 9(d) demonstrates an example of 3D multiphoton multicolour FISH in prenatal diagnosis. The 3D reconstruction from a set of multicolour images shows the intranuclear localization of the FISH-labelled centromeric regions of chromosomes 8 and 18 in an interphase nucleus of an amniotic fluid cell. The detection of three FITC signals in different planes indicates the presence of three chromosomes 18, suggestive of chromosomal abberation (Edward's syndrome).

5. Non-invasive optical biopsies

Besides multifluorophore excitation and optical sectioning, a further advantage of excitation radiation in the 700–1100 nm spectral range is the high light penetration depth due to the lack of efficient endogenous cellular absorbers and low scattering coefficients (Centonze & White, 1998). In principle, endogenous and exogenous fluorophores in thick samples, such as biopsies or living tissue, can be investigated to depths of more than 100 µm. Major depth limitations are the working distance of the objective, aberration phenomena, and multiple scattering. In turbid media with anisotropic scatterers, such as human tissues, multiple scattering of incident photons will induce a spatial and temporal dispersion of the excitation pulses and a subsequent signal reduction. Using a large-area detector (e.g. at the baseport), the effect of multiple scattered non-absorbed fluorescence photons on signal reduction can be minimized.

In order to get information of the spatial resolution and the signal intensity, we measured two-photon excited point spread functions (PSF) and signal-to-noise ratios (SNR) in fresh biopsies of human skin and of solid Ehrlich carcinoma mounted in phosphate buffered saline (PBS) using yellow-green fluorescent microbeads at various tissue depths. Using a 40× oil immersion objective, the PSF increased from

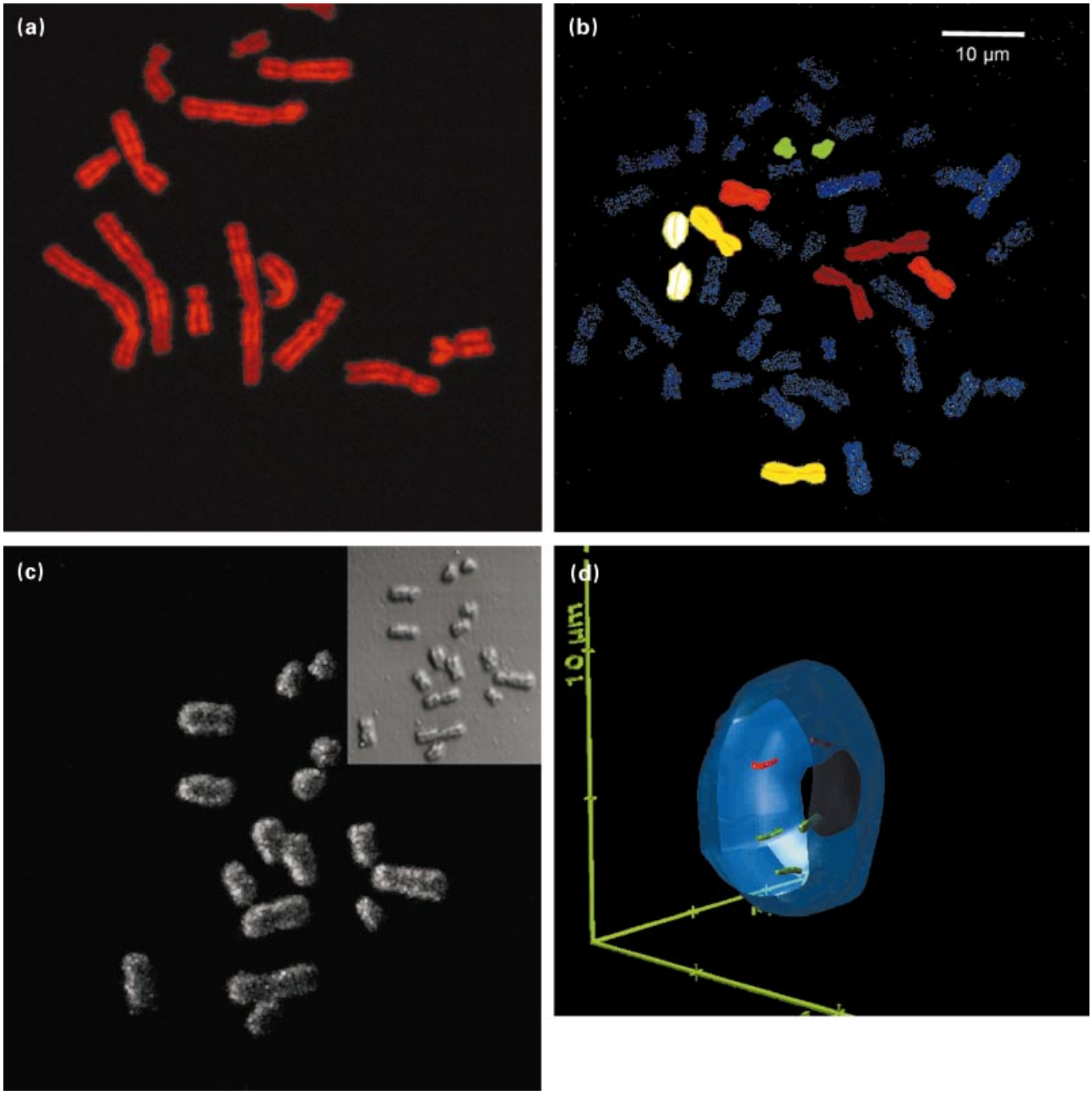

Fig. 9. Two-photon excited fluorescence of (a) DAPI-labelled human chromosomes. (b) Six-colour-FISH with the FISH fluorophores Spectrum Orange (white, chromosome 13), R110 (green, chromosome 21), Texas Red (yellow, chromosome 6), Cy 5 (red, chromosome 9), Cy 5.5 (dark red, chromosome 1) and DAPI (blue) (c) Giemsa-labelled chromosomes and (d) 3D reconstruction of the position of centromeric regions of chromosomes 8 (Rhodamine) and 18 (FITC) in the DAPI-labelled nucleus of amniotic fluid cell of a foetus with Edward's syndrome, based on optical sectioning. We applied two SP-750 filters to block IR excitation light.

values of 0.34 µm and 0.90 µm for radial and axial direction at 0 µm depth to values of 0.45 µm and 1.53 µm at 50 µm skin depth (Fig. 10a). As seen from Fig. 10(b), a typical increase in laser power by a factor of 10 is required to obtain the same SNR of bead fluorescence in 100 µm tumour tissue depth compared to beads at the surface. Therefore, fluorescence images with sufficient resolution can be obtained in deep tissue with moderate excitation powers.

NIR microscopy using cw laser sources and operation in the reflection mode has been used for fast *in vivo* imaging of human skin. However, fluorophores have not been detected with this system (Rajadhyaksha *et al.*, 1999). By contrast, multiphoton NIR autofluorescence microscopy provides a

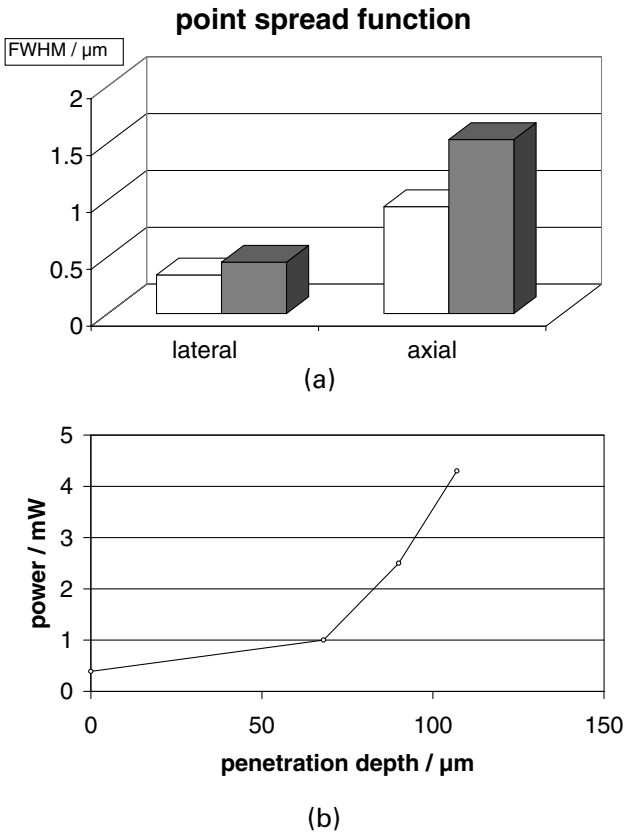

Fig. 10. (a) Two-photon point spread functions obtained from 3D images of 0.17 μm fluorescent latex spheres in human skin tissue at a depth of 50 μm (black) compared to beads on coverslip (white) without tissue. A 40× objective (NA = 1.30, mean working distance: 120 μm) and 170 fs pulses at 800 nm were used. (b) Mean power needed to maintain same SNR vs. tumour tissue depth.

method to obtain non-invasive optical biopsies with high spatial resolution and to perform morphological as well as functional imaging (Piston *et al.*, 1995; Masters *et al.*, 1997). In addition to coenzyme and elastic fibre imaging, detection of non-linearly excited melanin fluorescence has also been demonstrated (Teuchner *et al.*, 1999).

Figure 11 presents depth-dependent 730 nm excited autofluorescence images of fresh biopsies of human skin (breast) with emission maxima in the blue/green spectral range. Potential endogenous two-photon excitable fluorophores are NADH, NADPH, flavins and collagen. Intracellular structures, cell morphology and location of the nucleus in the different skin layers are clearly seen.

Preliminary *in vivo* autofluorescence imaging of the human forearm has been performed with a scan rate of $0.25\ s^{-1}$ (512×512 pixels). In addition to the oil immersion objective, measurements were also made with a water immersion objective (Zeiss, C Apochromat 40×, 1.2 W). High-resolution autofluorescence images along the entire 200 μm working distance can be obtained. However, it should be noted that the scan rate is limited due to the low fluorescence quantum yield of the endogenous fluorophores. Nevertheless, stacks of more than a hundred high contrast, motion-free autofluorescence images from different tissue depths have been obtained from patients without anaesthetic treatment. More rapid scanning is possible when exogenous fluorophores with a high fluorescence quantum yield are employed.

An example of *in vivo* fluorophore imaging is shown in Fig. 12, where the accumulation of protoporphyrin IX (PP IX) in tumour cells of mice with solid Ehrlich carcinoma has been detected. The excitation of the red-fluorescent porphyrin in the cytoplasm at 800 nm results also in excitation of endogenous blue/green-emitting fluorophores (NAD(P)H, flavins) associated with mitochondria. The use of special long-pass or broadband filters enables selective porphyrin imaging.

To my knowledge as yet no clinical trials have been conducted using multiphoton microscopes.

6. Multiphoton photochemistry in living cells

NIR radiation can induce the formation of reactive oxygen species (ROS) by non-linear excitation of photosensitizing molecules and subsequent type I or type II photo-oxidation processes. ROS-mediated lethal effects are used in photodynamic therapy (PDT) of tumours and other diseases (Doiron & Gomer, 1984). Typically, an exogenous photosensitizer such as the porphyrin mixture Photofrin with a high potential of singlet oxygen formation is applied to the target cells. Another well-known photosensitizer is PP IX, which is synthesized in the mitochondria of the tumour cells following uptake of the porphyrin precursor 5-aminolevulinic acid (ALA) (Kennedy *et al.*, 1990). Light excited porphyrin photosensitizers react with oxygen, mainly by a type II photo-oxidation process. Energy transfer occurs from the metastable triplet state to molecular oxygen and results in the formation of reactive singlet oxygen which induces cytotoxic effects. Although the major absorption band of the porphyrins is at around 400 nm, conventional porphyrin PDT is based on 633 nm radiation due to the higher light penetration depth. However, the absorption coefficient is about a factor of 30 less than the value at the major band at about 400 nm (Soret band, $\varepsilon = 6 \times 10^4\ M^{-1}\ cm^{-1}$, Photofrin in PBS). The application of intense NIR radiation at about 800 nm is an alternative approach to excite the porphyrin photosensitizers.

A number of efforts to use resonant or nonresonant two-photon excitation of photosensitizers have been reported. Andreoni *et al.* (1982) demonstrated sequential two-photon photoionization of haematoporphyrin. However, this resonant process requires UV or visible laser light. Experiments with 1.06 μm radiation of a Nd:YAG laser and the

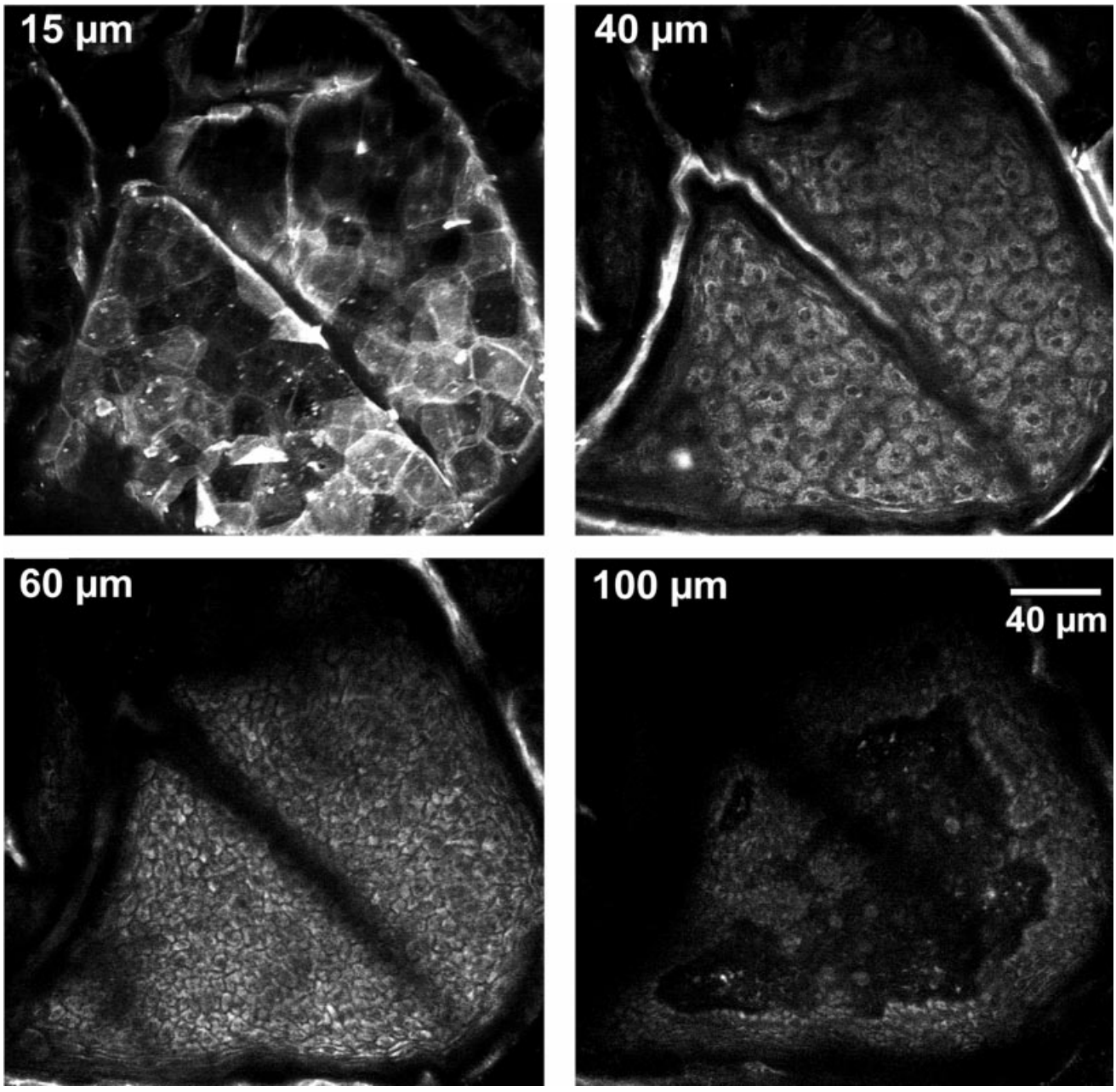

Fig. 11. Two-photon excited autofluorescence of human skin at different tissue depths.

photosensitizer Phaeophorbide led also to undesired thermal effects (Yamashita *et al.*, 1991).

Here we present data on the effect of 780 nm femtosecond laser scanning microscopy on the reproduction behaviour – a very sensitive indicator of cell damage – and vitality of Photofrin-labelled and ALA-labelled CHO cells. Cells were incubated with Photofrin for 12 h (5 $\mu g\ mL^{-1}$) and with ALA (1.5 $mg\ mL^{-1}$) for 4 h and exposed to 170 fs pulses at a mean power of 2 mW (130 W peak power, about 190 GW cm^{-2} peak intensity). A frame rate of 0.0625 s^{-1} (16 s $frame^{-1}$) was chosen. With a typical cellular area of 700 μm^2, the beam dwell time on one cell was $\approx$ 400 ms per scan. Subsequent scanning of Photofrin-labelled cells reduced cloning efficiency to 50% (only half of the cells show normal cell division) and to 0% (no reproduction) after about 13 scans ($\approx$10 mJ) and 50 scans, respectively. In the case of ALA incubation, about 24 scans and 100 scans were necessary. Live/dead assays revealed cytotoxic effects in most of the cells after 50 scans for Photofrin-labelled cells and 100 scans for ALA-labelled cells. The cell destruction was accompanied by fluorescence fading. Sensitizer-free control cells could be scanned more

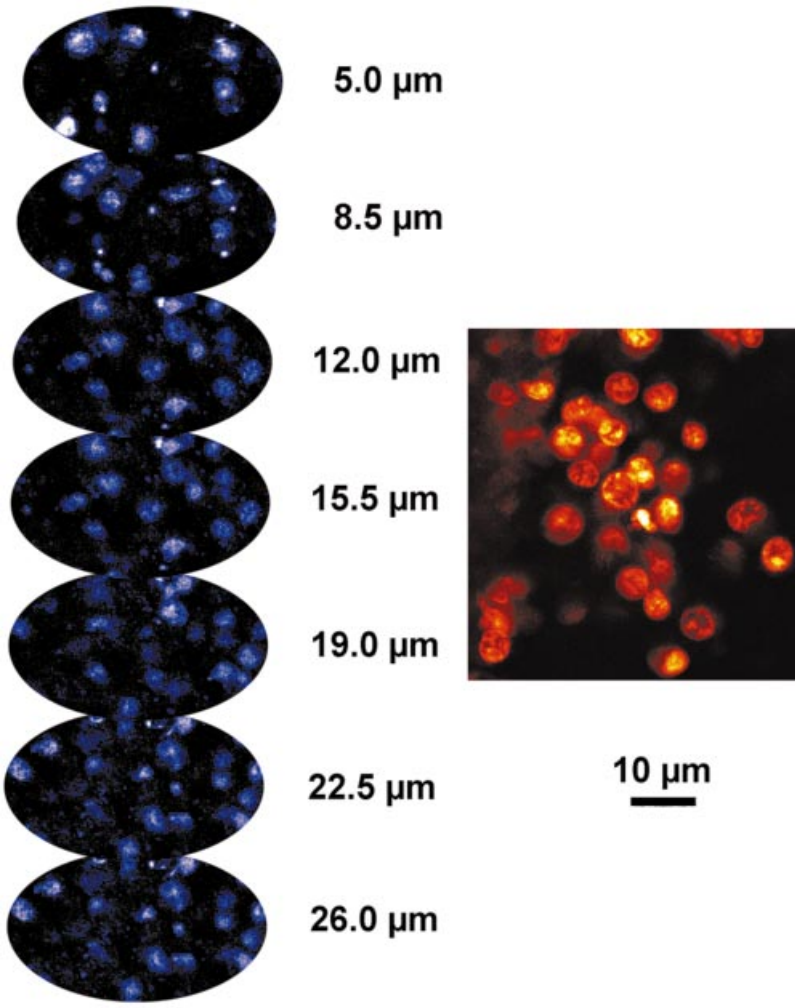

Fig. 12. Two-photon excited protoporphyrin in tumour tissue of a mouse with solid Ehrlich carcinoma.

than 700 times (4 h) without impact on the reproduction behaviour, morphology and vitality (Fig. 13) (König *et al.*, 1999c).

Two-photon excitation of intracellular porphyrins with NIR femtosecond pulses therefore seems an appropriate method to induce cell damage by photodynamic reactions. Major advantages of NIR porphyrin PDT are the excitation of higher order singlet states ('Soret band excitation'), the high light penetration depth of 780 nm radiation and the possibility to induce the desired effect highly localized within the three-dimensional target. Type I photodynamic therapy agents have also been excited by two-photon excitation with femtosecond laser pulses (Fisher *et al.*, 1997). The same group reported also on melanoma treatment using ultrashort NIR pulses (Wachter *et al.*, 1999). Further studies on NIR-exposed tissues and the development of new equipment for intense NIR illumination are necessary to perform PDT of cancer and other pathological disorders by non-resonant two-photon excitation.

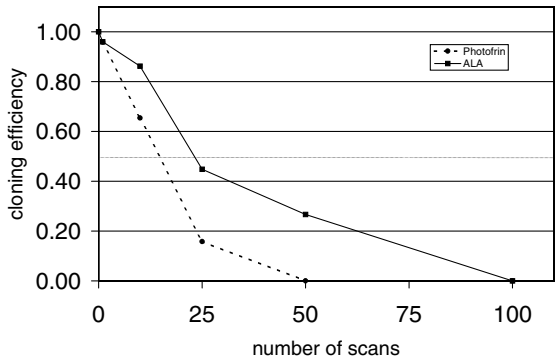

Fig. 13. Cloning efficiency of Photofrin-labelled and ALA-labelled cells vs. scan number after laser exposure with a 200 fs, 2 mW scanning beam at 60 µs pixel dwell time per scan.

Another two-photon induced photochemical effect is the highly localized photorelease of caged compounds with NIR laser radiation. The photorelease (photocleavage, uncaging) of bioactive substances, as well as of photolabile ion (Ca^{2+} and Mg^{2+})-specific chelators, have been reported (Denk

et al., 1990; Piston *et al.*, 1994; Brown *et al.*, 1999). Using two-photon femtosecond IR laser mediated photolysis of newly developed caged glutamate (Bhc-glu), Furuta *et al.* (1999) have recently obtained 3D maps of glutamate sensitivity of neurones in intact brain slices from rat cortex and hippocampus. Furthermore, Lipp & Niggli (1998) have used two-photon excitation photorelease of caged Ca^{2+} to spatially increase Ca^{2+} rapidly in extremely small volumes (10^{-15} L) of mammalian cardiac cells. Moreover, two-photon induced photorelease has also been employed for mapping the distribution of ligand-gated receptors in neuronal cells (Denk, 1994) and has been used to track the cell lines during development of sea urchin embryos (Summers *et al.*, 1996). Hence, the possibility to control highly local events in living cells with multiphoton photorelease and to image them with ultraprecise spatial resolution invariably constitutes an entirely new level in the study of cell signalling as well as in developmental biology.

7. Multiphoton microscopy in plant biology

In plants most of the light absorbed by photosynthetic pigments such as chlorophyll and carotenoids is utilized for photosynthetic quantum conversion, while only a small portion is de-excited through emission as red and far-red chlorophyll fluorescence. The red and far-red chlorophyll emission spectrum is characterized by two maxima near 690 nm and 740 nm. The fluorescence induced by a 355 nm Nd:YAG laser has been used for detection of stress-induced changes in the red and far-red fluorescence emission (Lichtenthaler & Miehe, 1997). We have instead successfully employed femtosecond NIR pulses at 800 nm to detect chlorophyll autofluorescence in intact root hypocotyl (Fig. 14a and b) and in leaf epidermis (Fig. 14c and d). Hence, with multiphoton fluorescence microscopy one can assess the photosynthetic performance of a single cell deep in the green plant tissue (Tirlapur & König, recent unpublished results). It is equally interesting to note that in the hypocotyl, in addition to the chloroplasts, the cell walls also show autofluorescence when excited at 800 nm. Similar cell wall associated autofluorescence can be seen following UV excitation, and it is generally believed to be due to blue-green fluorescing ferulic acid covalently bound to cell walls (Buschmann & Lichtenthaler, 1998). While chlorophyll can potentially be excited by far-red wavelengths by a one-photon process, 800 nm excited chlorophyll fluorescence followed a squared relation on laser power, indicating a two-photon process.

The green fluorescent protein (GFP), a novel marker protein derived from the jellyfish *Aequorea victoria*, with its autofluorescence characteristics, has proved to be invaluable in the study of gene expression, trafficking and organelle structure within living cells. GFP has been targeted to various cell organelles such as the nucleus, endoplasmic reticulum, Golgi and plastids (Haseloff & Siemering, 1998; Llopis *et al.*, 1998; Tirlapur *et al.*, 1999). In most of these studies the subcellular localization of the fusion protein in living cells has been monitored by a conventional confocal laser scanning microscope using the 488 nm laser line. Wild type GFP emits green (maximum 508 nm). Recently, GFP-expressing neuronal cells have been imaged by two-photon microscopy (Mainen *et al.*, 1999). Similarly, using NIR femtosecond laser radiation at 780 nm and 800 nm we have been able to image endoplasmic reticulum (ER) as well as plastid targeted GFP in intact living root (Fig. 15a and b) and in the stomatal guard cells (Fig. 15c and d) of an etiolated leaf in *Arabidopsis.*

Besides the use of multiphoton microscopy for fluorescence imaging it can aslo be used for non-invasive introduction of various probes into living plant cells. Intracellular transport of macromolecules between plant cells occurs symplastically through plasmodesmata. Knowledge pertaining to symplastic communication in plants is often analysed by visualizing the cell-to-cell movement of plasma membrane-impermeable fluorescent dyes. Usually the dye is introduced into a single cell by application of invasive microinjection methods (Goodwin *et al.*, 1990). However, the microinjection technique cannot be used to introduce fluorescent dye in a single cell that is deep in the plant tissue. In complete contrast to physical intrusion with a microinjection needle, a novel non-invasive technique based on NIR femtosecond laser pulses for dye permeation and 3D imaging of dye coupling (Fig. 15e–g) between different cell types in the root meristem of *Arabidopsis* has been developed (Tirlapur & König, 1999). Because the NIR-laser based approach is highly efficient it has a number of potential applications for non-contact, non-invasive loading of fluorescent probes in a wide range of cell types as well as in studies addressing cell–cell communication.

8. Cell damage in multiphoton microscopes

As described in section 6, femtosecond laser microscopy of living specimens can be performed with a peak intensity of about 200 GW cm^{-2} for hours without impact on cellular reproduction and vitality. Squirrel *et al.* (1999) exposed hamster embryos for 24 h to NIR femtosecond laser pulses of a multiphoton fluorescence microscope without impact on embryo development, in contrast to conventional one-photon laser scanning microscopy.

However, non-destructive multiphoton imaging of living specimens is confined to a particular optical window. The lower limitation is determined by the optical properties of the fluorophore (e.g. molecular multiphoton absorption cross-section and fluorescence quantum yield) and by the detector sensitivity, the upper by the onset of cell damage.

We investigated the influence of cw and ultrashort laser

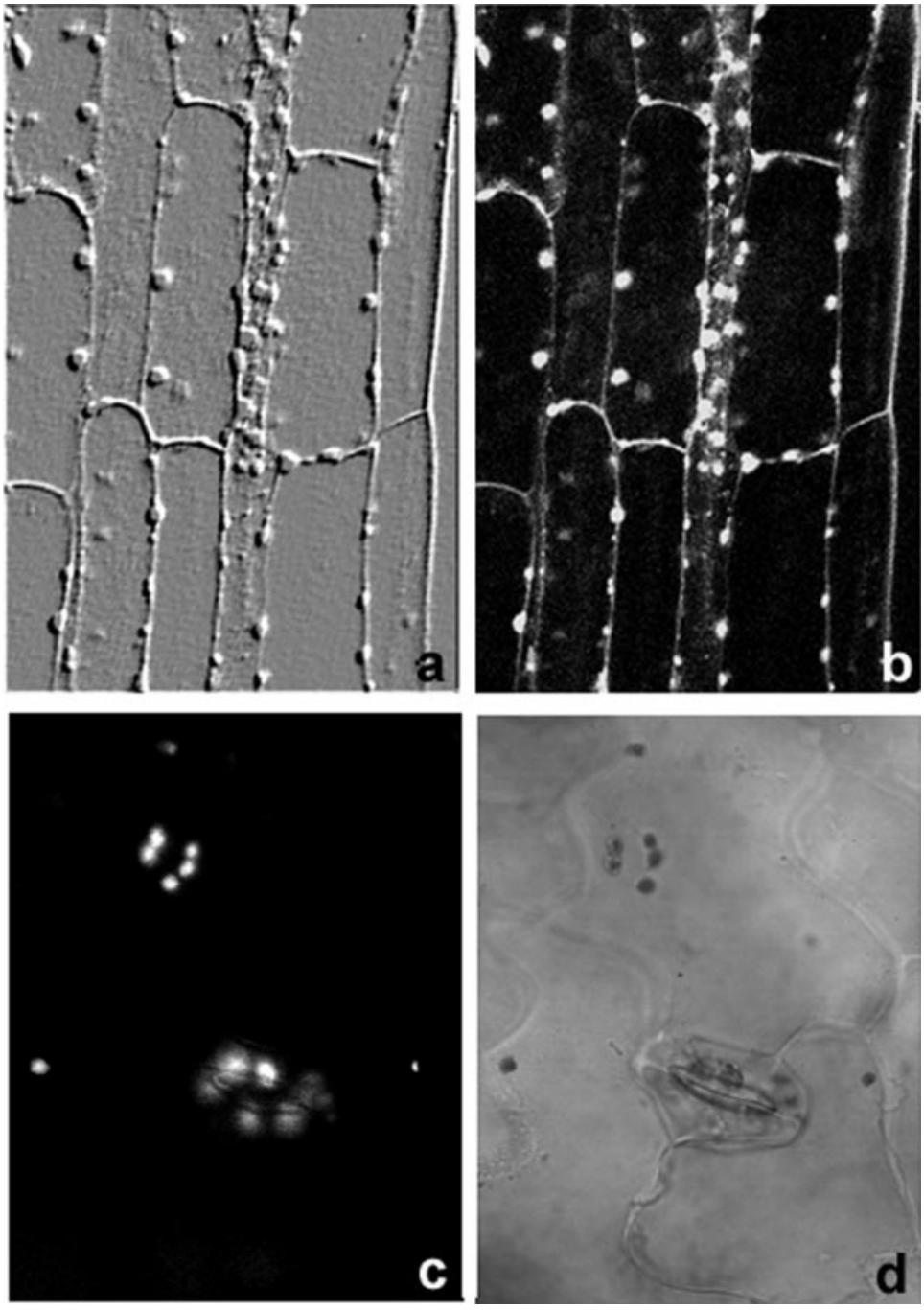

Fig. 14. Two-photon excited chlorophyll autofluorescence in hypocotyl (a and b) and leaf epidermal cells (c and d) of *Arabidopsis* induced with 800 nm laser pulses. Image a is generated by emboss filtering from fluorescence data.

pulses at different NIR wavelength, power and pulse width on the metabolism, reproduction behaviour and vitality of CHO cells. Cells were exposed 10 times to a highly focused scanning with 80 μs beam dwell time per pixel (König *et al.*, 1996b,c, 1997, 1999).

For the same pulse energy, photodamage was found to be more pronounced at shorter pulses. At 780 nm, cw scanning beams did not harm cells up to 35 mW power, whereas 2 ps pulses induced loss of viability at 22 mW mean power. Impaired cell division was found for half of the 2 ps exposed cells at 11 mW mean power (P_{50}). By contrast, 240 fs pulses led to 50% cloning efficiency and cell death at mean powers of 3 and 7 mW, respectively (Fig. 16). Using laser powers of 2 mW or less, CHO cells

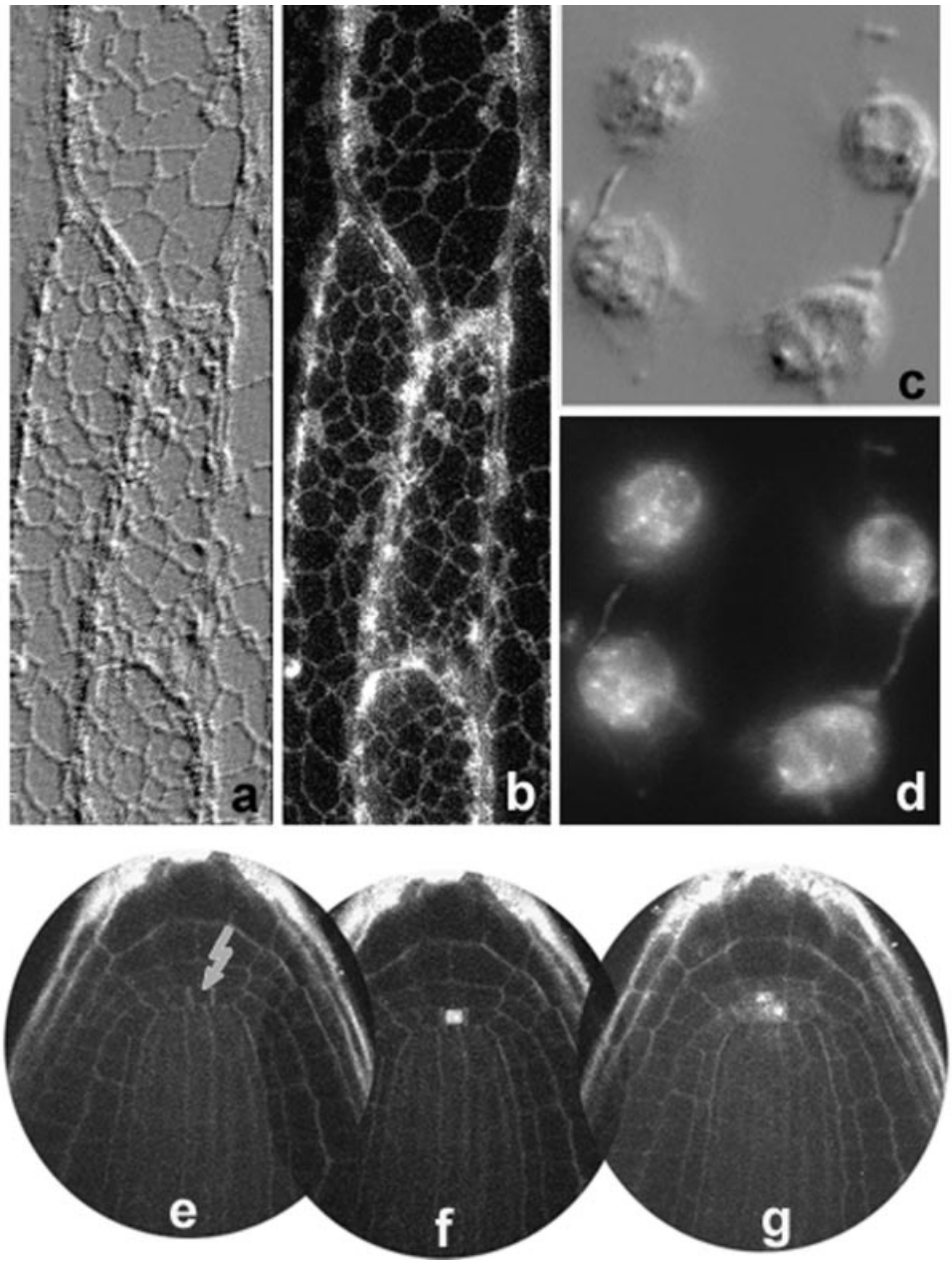

Fig. 15. Imaging of two-photon excited GFP fluorescence in plant cells expressing ER- (a and b) and plastid- (c and d) targeted GFP. Time-lapse imaging of dye coupling in *Arabidopsis* root tip (e: 0 s, f: 8 s, g: 2 min) following NIR laser mediated dye permeation in a single central cell. Images (a) and (c) were obtained by emboss filtering.

could be scanned more than 700 times without impact on the reproduction. There is therefore no simple relation between photodamage and energy density. Below certain power (intensity) thresholds, 'safe' multiphoton microscopy appears possible.

According to the smaller image in Fig. 16, where the P_{50} values vs. the root of the pulse broadening are depicted, the photodamage process is probably based on a two-photon excitation process rather than a one-photon or three-photon event. This is consistent with the findings that the cell damage at 920 nm was less pronounced than at 780 nm where water absorbs less. Photodamage is therefore not based on linear water heating. This was also shown in cw 1064 nm microbeam studies where CHO cells, labelled with a thermosensitive fluorophore, were exposed to MW cm^{-2} intensities and GJ cm^{-2} fluence, as well as by temperature calculations in the case of exposure to fs and ps pulses (Liu *et al.*, 1995; Schönle & Hell, 1998).

Using 780 nm pulses, three-photon absorption may result in nuclear DNA excitation due to the major

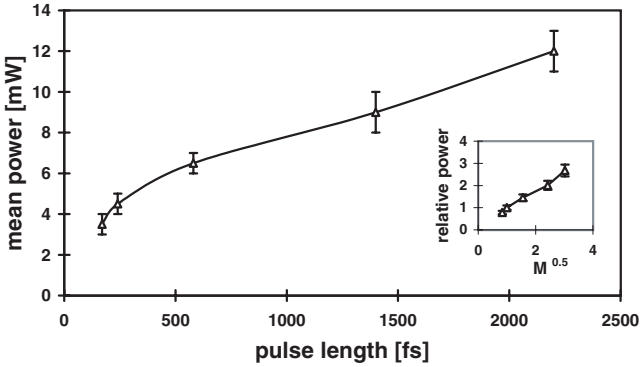

Fig. 16. Photodamage resulting from exposure to femtosecond and picosecond laser pulses. The mean powers of 780 nm pulses to induce failed cellular reproduction of half the laser-exposed CHO cells (50% cloning efficiency) vs. pulse width is shown. In the smaller included image, the relative mean power vs. squared root of pulse broadening M is shown. The damage process follows approximately a P^2/τ relation.

absorption band of nucleic acids at 260 nm. However, photoinduced cell damage such as failed reproduction was also obtained when light exposure was restricted to intracellular regions outside the nucleus.

The findings that photodamage seems to be based on a two-photon excitation process has the consequence that picosecond as well as femtosecond pulses are appropriate sources of two-photon microscopy. Because of the same P^2/τ dependence of damage and fluorescence, the ratio (typically 1–30) of minimum powers to induce cell damage and to excite fluorescence via a two-photon absorption process is the same for picosecond and femtosecond laser pulses. It makes therefore no sense to use high-cost pulse compression units. By contrast, in three-photon imaging, which requires higher photon flux densities due to a P^3/τ^2 relation, the relative window will be narrower and will decrease with increasing pulse length. In this case, fs pulses are appropriate sources in the case of efficient non-destructive three-photon imaging.

In order to compare the photodamage in NIR multiphoton microscopes vs. UV one photon microscopes, the same assay was performed on CHO cells using a 364-nm scanning beam of a conventional laser scanning microscope with an Ar^+ laser. A 50% cloning efficiency was obtained at the low power of 4 μW. Therefore, UV-induced damage occurs at about three orders lower powers (4 μW) compared to the mean values of NIR femtosecond laser pulses (2–8 mW).

With respect to the excitation wavelength, the photodamage can be based on two-photon absorption by endogenous cellular absorbers, such as by the coenzymes NAD(P)H and flavins as well as by porphyrins. It is well-known that excitation of these endogenous photosensitizers can result in the formation of ROS (oxidative stress) and indirect DNA damage (Tyrell & Keyse, 1990; Cunningham *et al.*, 1985). The major localization site of the coenzymes is the mitochondria. Our ultrastructural studies reveal that these organelles are the major targets of NIR irradiation. Laser exposure resulted in swollen mitochondria accompanied by loss of christae combined with the formation of electron-dense bodies in the mitochondrial matrix (Oehring *et al.*, 2000).

ROS play an important role in apoptosis. We found NIR-induced apoptosis-like cell death. In particular, changes in cytoplasmic and nuclear calcium levels, fragmentation of F-actin cytoskeleton, disruption of plasma membrane integrity and morphological deformations of the nuclei and nuclear envelope following exposure with 170 fs laser pulses with powers higher than 7 mW have been detected (Tirlapur & König, recent unpublished results).

On increasing the power levels to values higher than 10 mW, another destructive effect may occur. The use of very high light intensities in the TW cm^{-2} region induces intracellular optical breakdown and plasma formation accompanied by intense white luminescence and complex sub-nanosecond emission decay kinetics (König *et al.*, 1996c). Scanning at these light intensities results in severe shockwave-induced morphological damage, such as cell fragmentation. Typically, cells die immediately.

In conclusion, multiphoton fluorescence imaging appears to be a safe novel optical sectioning technique within a particular intensity window. Above the threshold, failed reproduction and apoptosis-like lethal effects probably based on two-photon photochemical photodamage as well as on immediate cell damage via optical breakdown may occur.

9. Nanosurgery

If the mean power in 80 MHz femtosecond laser microscopes with high numerical aperture objectives is increased to 30–50 mW, light intensities of TW cm^{-2} can be used for material processing based on plasma-induced ablation. The threshold for optical breakdown is lower for biological material than for water and cell culture medium and was found to be lowest in the perinuclear region of cells. We used the modes of ROI scanning, line scan and single spot illumination to knock out intracellular material, to perform dissections (König *et al.*, 1999b) and to 'drill' holes.

By fine tuning of the laser power only the central part of the beam spot can provide sufficient intensity for material removal. It is therefore possible to drill holes and to cut structures with a precision below the diffraction-limited submicrometre beam spot. We used the multiphoton-induced ablation process to cut human chromosomes. Measurements with the force scanning microscope reveal chromosome dissection with a cut size below 300 nm. In addition, partial removal (incisions) of chromosome material with a precision of 110 nm was obtained (Fig. 17). The

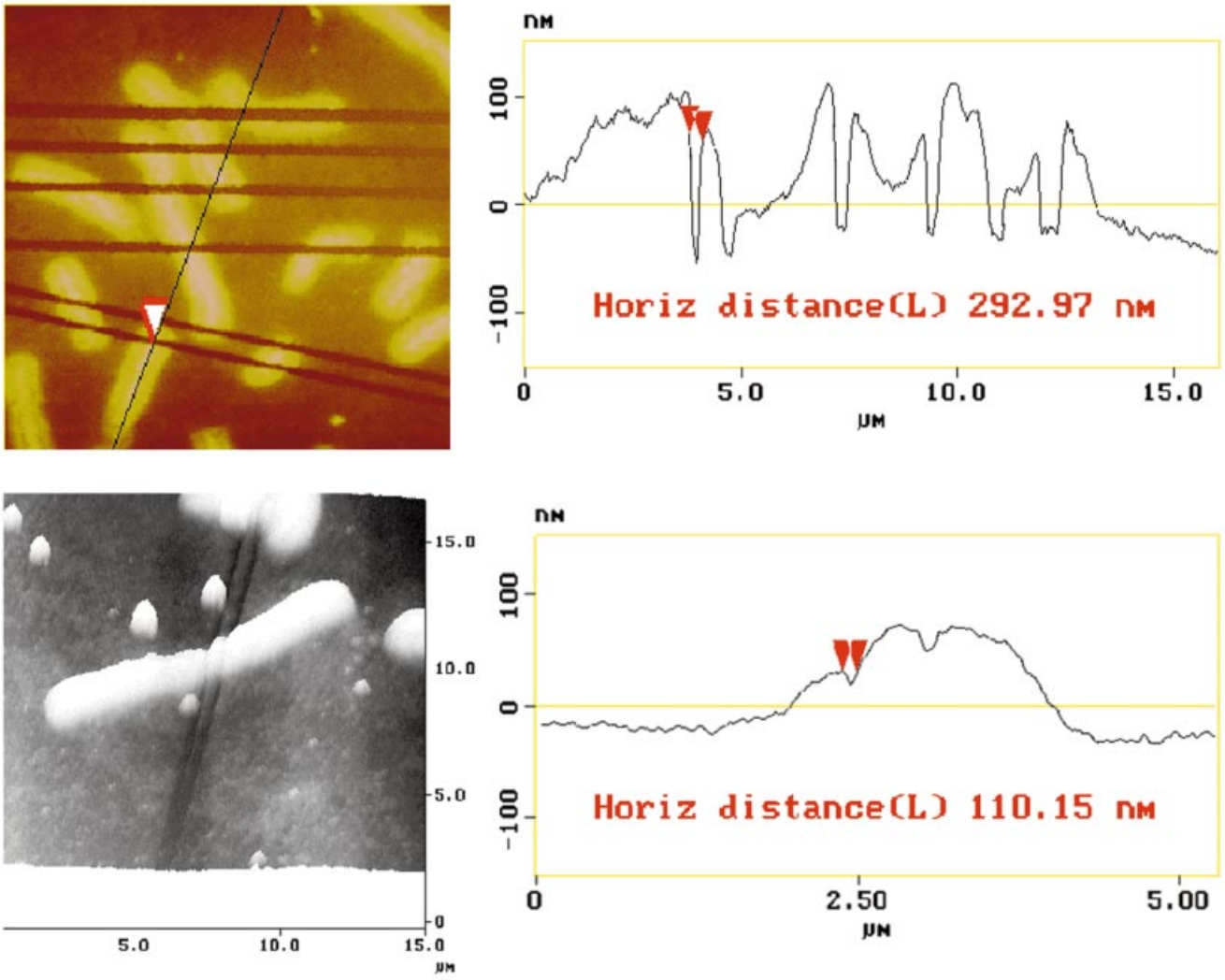

Fig. 17. Nanodissection of chromosomes with 170 fs pulses at 800 nm and 80 MHz. A cut size of 110–290 nm was measured with the force scanning microscope.

figure demonstrates probably the smallest laser cuts in biological materials. The femtosecond laser microscopy opens the possibility to provide a non-contact nanoscalpel for surgery inside the cell, cell nucleus or organelle without affecting other cellular compartments. We were able to cut chromosomes within a living cell (Fig. 18). The cells remained alive and completed cell division after laser surgery.

In conclusion, femtosecond NIR laser pulses with their advantages of high penetration depth, no out-of-focus absorption, efficient induction of multiphoton processes, post-pulse material removal, absence of plasma shielding effects and of significant heat transfer appear the appropriate choice for intracellular surgery. In contrast to laser microsurgery formerly performed in living cells with UV and visible lasers at typically nanosecond pulse width (Bessis *et al.*, 1962; Berns *et al.*, 1969; Berns, 1974; Greulich *et al.*, 1989; Greulich & Weber, 1992; Schütze *et al.*, 1994; Berns, 1998; Greulich, 1999), NIR nanosurgery with ultrashort laser pulses provides higher precision, and the possibility to treat structures deep within the tissue and to avoid severe damage to surrounding structures.

10. Conclusions

NIR multiphoton excitation laser scanning microscopes provide attractive advantages over conventional fluorescence microscopes and can be employed as novel non-contact biomedical tools for three-dimensionally resolved fluorescence imaging, optical diagnostics, photochemistry and nanoprocessing within submicrometre domains of biomolecules and living cells. Because multiphoton excitation at high intensities occurs only in the minute focal volume of a high numerical aperture objective it inherently

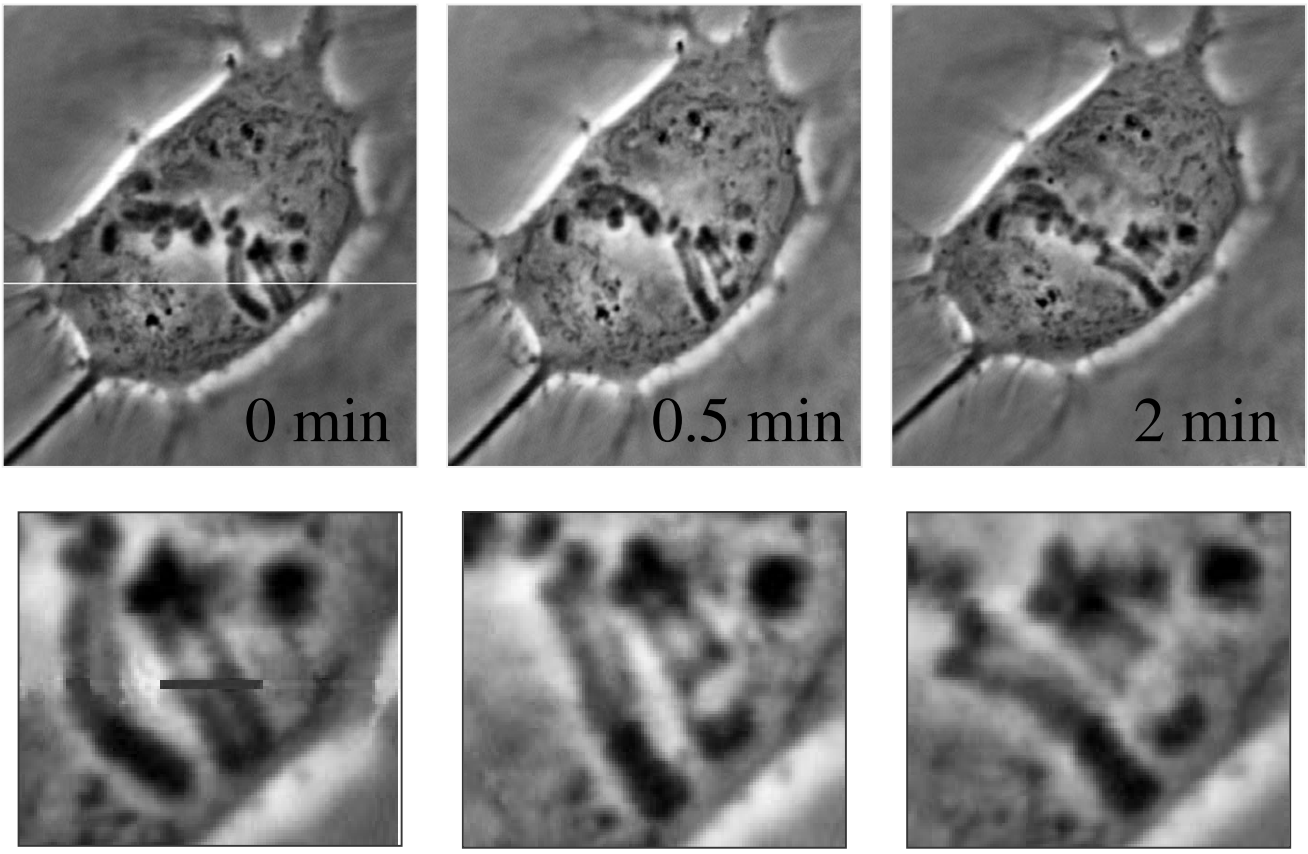

Fig. 18. Chromosome dissection within living cells using the femtosecond NIR laser microscope. The cell remained alive.

provides three-dimensional resolution, while photobleaching and photodamage are minimized in out-of-focus regions. These advantages allow experiments on thick living samples for 3D fluorescence diagnostics with sub-nanosecond and sub-micrometre resolution, DNA and live cell studies, and to acquire optical biopsies. Furthermore, these novel microscopes have versatile applications for photodynamic inactivation of tumour cells, release of photolabile caged compounds and intracellular nanosurgery. It is therefore conceivable that future technical advances will continue to increase the range of applicability of multiphoton laser scanning microscopes in biomedical and biotechnological sciences.

Acknowledgements

The author thanks Professor K-J. Halbhuber, Dr I. Riemann, Dr P. Fischer (Institute of Anatomy II, University of Jena) and Dr W. Fritzsche (IPHT Jena) for scientific support and Dr U. K. Tirlapur for constructive comments and for critically reading this manuscript. The financial support from Carl Zeiss Jena GmbH, the German Science Foundation (DFG) and the Federal Ministry of Education, Science, Research and Technology (BMBF) is gratefully acknowledged.

References

Andreoni, A., Cubeddu, R., De Silverstri, S., Laporta, P. & Svelto, O. (1982) Two-step laser activation of hematoporphyrin derivative. *Chem. Phys. Lett.* **88**, 37–39.

Ashkin, A. & Dziedzik, J.M. (1987) Optical trapping and manipulation of viruses and bacteria. *Science*, **235**, 1517–1520.

Berns, M.W. (1974) *Biological Microirradiation. Classical and Laser Sources.* Prentice Hall, Englewood Cliffs, New Jersey.

Berns, M.W. (1998) Laser scissors and tweezers. *Sci. Am.* **278**, 62–67.

Berns, M.W., Olson, R.S. & Rounds, D.E. (1969) *In vitro* production of chromosomal lesions using an argon ion laser microbeam. *Nature*, **221**, 74–75.

Bessis, M., Gires, F., Mayer, G. & Normaski, G. (1962) Irradiation des organites cellulaires a l'aide d'un laser a rubis. *C. R. Acad. Sci.* **255**, 1010–1012.

Bewersdorf, J., Pick, R. & Hell, S.W. (1998) Multifocal multiphoton microscopy. *Opt. Lett.* **23**, 655–657.

Block, S.M., Blair, D.F. & Berg, H.C. (1989) Compliance of bacterial flagella measured with optical tweezers. *Nature*. **338**, 514–518.

Booth, M. & Hell, S.W. (1998) Continuous wave excitation

two-photon fluorescence microscopy exemplified with the 647 nm ArKr laser line. *J. Microsc.* **190**, 298–304.

Brown, E.B., Shear, J.B., Adams, S.R., Tsien, R.Y. & Webb, W.W. (1999) Photolysis of caged calcium in femtoliter volumes using two-photon excitation. *Biophys. J.* **76**, 489–499.

Buschmann, C. & Lichtenthaler, H.K. (1998) Principles and characteristics of multi-color fluorescence imaging of plants. *J. Plant Physiol.* **152**, 297–314.

Centonze, V.E. & White, J.G. (1998) Multiphoton excitation provides optical sections from deeper within scattering specimens than confocal imaging. *Biophys. J.* **75**, 2015–2024.

Chu, S. (1991) Laser manipulation of atoms and particles. *Science*, **253**, 861–866.

Cunningham, M.L., Johnson, J.S., Giovanazzi, S.M. & Peak, M.J. (1985) Photosensitised production of superoxide anion by monochromatic (290–405 nm) ultraviolet irradiation of NADH and NADPH coenzymes. *Photochem. Photobiol.* **42** (2), 125–128.

Denk, W. (1994) Two-photon scanning photochemical microscopy: mapping ligand-gated ion channel distribution. *Proc. Natl. Acad. Sci. USA.* **91**, 6629–6633.

Denk, W., Piston, D.W. & Webb, W.W. (1995) Two-photon molecular excitation in laser-scanning microscopy. *Handbook of Biological Confocal Microscopy.* 2nd edn (ed. by J. B. Pawley), pp. 445–458. Plenum Press, New York.

Denk, W., Strickler, J.H. & Webb, W.W. (1990) Two-photon laser scanning microscope. *Science*, **248**, 73–76.

Doiron, D.R. & Gomer, C.J. (1984) *Porphyrin Localisation and Treatment of Tumours.* Alan R. Liss, New York.

Fan, G.Y., Fujisaki, H., Miyawaki, A., Tsay, R.K., Tsien, R.Y. & Ellisman, M.H. (1999) Video-rate scanning two-photon excitation fluorescence microscopy and ratio imaging with chameleons. *Biophys. J.* **76**, 2412–2420.

Fisher, W.G., Partridge, W.P., Dees, C. & Wachter, E.A. (1997) Simultaneous two-photon activation of type I photodynamic therapy agents. *Photochem. Photobiol.* **66**, 141–155.

Furuta, T., Wang, S.S.-H., Dantzker, J.L., Dore, T.M., Bybee, W.J., Callaway, E.M., Denk, W. & Tsien, R.Y. (1999) Brominated 7-hydroxycoumarin-4-ylmethyls: photolabile protecting groups with biologically useful cross-sections for two photon photolysis. *PNAS (USA)*, **96**, 1193–1200.

Goodwin, P.B., Shepherd, V. & Erwee, M.G. (1990) Compartmentation of fluorescent tracers injected into the epidermal cells of *Egeria densa* leaves. *Planta*, **181**, 129–136.

Göppert-Meyer, M. (1931) Über Elementarakte mit zwei Quantensprüngen. Göttinger Dissertation. *Ann. Phys.* **9**, 273–294.

Greulich, K.O. (1999) *Micromanipulation by Light in Biology and Medicine.* Birkhäuser, Basel.

Greulich, K.O., Bauder, U., Monajembashi, S., Ponelies, N., Seeger, S. & Wolfrum, J. (1989) Laser microbeam and optical tweezers. *Labor*, **2000**, 36–46(in German).

Greulich, K.O. & Weber, G. (1992) The light microscope on its way from an analytical to a preparative tool. *J. Microsc.* **167**, 127–151.

Gu, M. & Day, D. (1999) Two-photon multilayer bit data storage by use of continuous wave illumination. *SPIE Proceed.* **3749**, 444–445.

Hale, G.M. & Querry, M.R. (1973) Optical constants of water in the 200-nm to 200-mm wavelength region. *Appl. Opt.* **12**, 555–563.

Hänninen, P.E., Schrader, M., Soini, E. & Hell, S.W. (1995) Two-photon excitation fluorescence microscopy using a semiconductor laser. *Bioimaging*, **3**, 70–75.

Hänninen, P.E., Soini, E. & Hell, S.W. (1994) Continuous wave excitation two-photon fluorescence microscopy. *J. Microsc.* **176**, 222–225.

Haseloff, J. & Siemering, K.R. (1998) The uses of GFP in plants. *Green Fluorescent Protein. Strategies, Applications and Protocols* (ed. by M. Chalfie & S, Kain), pp. 191–220. Wiley, New York.

Hell, S.W., Booth, M., Wilms, S., Schnetter, C.M., Kirsch, A.K., Arndt-Jovin, D.J. & Jovin, T. (1998) Two-photon near and far-field fluorescence microscopy with continuous-wave excitation. *Opt. Lett.* **23**, 1238–1240.

Hell, S.W., Schrader, M. & van der Voort, H.T.M. (1997) Far-field fluorescence microscopy with three-dimensional resolution in the 100-nm range. *J. Microsc.* **187**, 1–7.

Hell, S.W. & Stelzer, E.H.K. (1992) Fundamental improvement of resolution with a 4Pi-confocal fluorescence microscope using two-photon excitation. *Opt. Commun.* **93**, 277.

Jenei, A., Kirsch, A.K., Subramaniam, V., Arndt-Jovin, D. & Jovin, T.M. (1999) Picosecond multiphoton scanning near-field microscopy. *Biophys. J.* **76**, 1092–1100.

Kaiser, W. & Garret, C. (1961) Two-photon excitation in CaF_2: Eu^{2+}. *Phys. Rev. Lett.* **7**, 229–231.

Kennedy, J.C., Pottier, R.H. & Pross, D.C. (1990) Photodynamic therapy with endogenous protoporphyrin IX: basic principles and present clinical experience. *J. Photochem. Photobiol. B*, **6**, 143–148.

Kirsch, A.K., Subramaniam, V., Striker, G., Schnetter, C., Arndt-Jovin, D. & Jovin, T.M. (1998) Continuous wave two-photon scanning near-field optical microscopy. *Biophys. J.* **75**, 1513–1521.

König, K. (1997) Two-photon near-infrared excitation in living cells. *J. Near Infrared Spectrosc.* **5**, 27–34.

König, K. (1999) *Optische Mikromanipulation und Zweiphotonen-Anregung Vitaler Zellen Mittels Naher Infrarot Mikroskopie.* Shaker-Verlag, Aachen, Germany.

König, K., Becker, T.W., Fischer, P., Riemann, I. & Halbhuber, K.J. (1999a) Pulse-length dependence of cellular response to intense near-infrared laser pulses in multiphoton microscopes. *Opt. Lett.* **24**, 113–115.

König, K., Boehme, S., Leclerc, N. & Ahuja, R. (1998) Time-gated autofluorescence microscopy of motile green microalga in an optical trap. *Cell. Mol. Biol.* **44**, 763–770.

König, K., Göhlert, A., Liehr, T., Loncarevic, I.F. & Riemann, I. (2000) Two-Photon Multicolour FISH: a versatile technique to detect specific sequences within single DNA molecules in cells and tissues. *Single Mol.* **1**, 41–51.

König, K., Krasieva, T., Bauer, E., Fiedler, U., Berns, M.W., Tromberg, B.J. & Greulich, K.O. (1996a) Cell damage by UVA radiation of a mercury microscopy lamp probed by autofluorescence modifications, cloning assay, and comet assay. *J. Biomed. Optics*, **1** (2), 217–222.

König, K., Liang, H., Berns, M.W. & Tromberg, B.J. (1995) Cell damage by near-IR microbeams. *Nature*, **377**, 20–21.

König, K., Liang, H., Berns, M.W. & Tromberg, B.J. (1996b) Cell

damage in near infrared multimode optical traps as a result of multiphoton absorption. *Opt. Lett*. **21**, 1090–1092.

König, K., Riemann, I. & Fischer, P. (1999c) Photodynamic therapy by non-resonant two-photon excitation. *SPIE Proceed*. **3592**, in press.

König, K., Riemann, I., Fischer, P. & Halbhuber, K.J. (1999b) Intracellular nanosurgery with near infrared femtosecond laser pulses. *Cell. Mol. Biol*. **45**, 195–201.

König, K., Simon, U. & Halbhuber, K.J. (1996d) 3D resolved two-photon fluorescence microscopy of living cells using a modified confocal laser scanning microscope. *Cell. Mol. Biol*. **42**, 1181–1194.

König, K., So, P.T.C., Mantulin, W.W., Tromberg, B.J. & Gratton, E. (1996c) Two-photon excited lifetime imaging of autofluorescence in cells during UVA and NIR photostress. *J. Microsc*. **183**, 197–204.

König, K., So, P., Mantulin, W.W., Tromberg, B.J. & Gratton, E. (1997) Cellular response to near infrared femtosecond laser pulses in two-photon microscopes. *Opt. Lett*. **22**, 135.

Lichtenthaler, H.K. & Miehe, J.A. (1997) Fluorescence imaging as a diagnostic tool for plant stress. *Trends Plant Sci*. **2**, 316–320.

Lipp, P. & Niggli, E. (1998) Fundamental calcium release events revealed by two-photon excitation photolysis of caged calcium in guinea-pig cardiac myocytes. *J. Physiol*. **508**, 801–809.

Llopis, J., McCaffery, J.M., Miyawaki, A., Farquhar, M.G. & Tsien, R.Y. (1998) Measurement of cytosolic, mitochondrial, and Golgi pH in single living cells with green fluorescent protein. *Proc. Natl. Acad. Sci. USA*, **95**, 6803–6808.

Mackville, M., Veldman, T., Padilla-Nash, H., Wangsa, D., O'Brien, P., Schröck, E. & Ried, T. (1997) Spectral karyotyping, a 24-colour FISH techique for the identification of chromosomal rearrangements. *Histochem. Cell Biol*. **108**, 299–303.

Mainen, Z.F., Maletic-Savatic, M., Shi, S.H., Hayashi, Y., Mailinow, R. & Savoboda, K. (1999) Two-photon imaging in living brain slices. *Methods*, **18**, 231–239.

Maiti, S., Shear, J.B., Williams, R.M., Zipfel, W.R. & Webb, W.W. (1997) Measuring serotonin distribution in live cells with three-photon excitation. *Science*, **275**, 530–532.

Masters, B.R., So, P.T.C. & Gratton, E. (1997) Multiphoton excitation fluorescence microscopy and spectroscopy of *in vivo* human skin. *Biophys. J*. **72**, 2405–2412.

Minsky, M. (1988) Memories on inventing the confocal scanning microscope. *Scanning*, **10**, 128–138.

Nederlof, P.M., Robinson, D., Abuknesha, R., Wiegant, J., Hopmann, A.H., Tanke, H.J. & Raap, A.K. (1989) Three color fluorescence *in situ* hybridization for the simultaneous detection of multiple nucleic acid sequences. *Cytometry*, **10**, 20–27.

Oehring, H., Riemann, I., Fischer, P., Halbhuber, K.J. & König, K. (2000) Ultrastructure and reproduction behaviour of single CHO-K1 cells exposed to near infrared femtosecond laser pulses. *Scanning*, **22**, 263–270.

Pawley, J.B., ed. (1995) *Handbook of Biological Confocal Microscopy*. 2nd edn. Plenum Press, New York.

Perkins, T.T., Quake, S.R., Smith, D.E. & Chu, S. (1994b) Relaxation of a single DNA molecule observed by optical microscopy. *Science*, **264**, 822–826.

Perkins, T.T., Smith, D.E. & Chu, S. (1994a) Direct observation of tube-like motion of a single polymer chain. *Science*, **264**, 819–822.

Piston, D.W., Kirby, M.S., Cheng, H. & Lederer, W.J. (1994) Two-photon excitation fluorescence imaging of three-dimensional calcium-ion activity. *Appl. Opt*. **33**, 662–669.

Piston, D.W., Masters, B.R. & Webb, W.W. (1995) Three-dimensionally resolved NAD (P) H cellular metabolic redox imaging of the *in situ* cornea with two-photon excitation laser scanning microscopy. *J. Microsc*. **178** (1), 20–27.

Rajadhyaksha, M., Gonzales, S., Zavislan, J.M., Anderson, R.R. & Webb, R.H. (1999) *In vivo* confocal laser microscopy of human skin. II: advances in instrumentation and comparison with histology. *J. Invest. Dermatol*. **113**, 293–303.

Ried, T., Baldini, A., Rand, T.C. & Ward, D.C. (1992) Simultaneous visualization of seven different DNA probes by *in situ* hybridization using combinatorial fluorescence and digital imaging microscopy. *Proc. Natl. Acad. Sci. USA*, **89**, 1388–1392.

Sako, Y., Sekihata, A., Yanagisawa, Y., Yamamoto, M., Shimada, Y., Ozaki, K. & Kusumi, A. (1997) Comparison of two-photon excitation laser scanning microscopy with UV-confocal laser scanning microscopy in 3D calcium imaging using the fluorescence indicator Indo-1. *J. Microsc*. **185**, 9–20.

Schönle, A. & Hell, S. (1998) Heating by absorption in the focus of an objective lens. *Opt. Lett*. **23**, 325.

Schrader, M., Bahlmann, K., Giese, G. & Hell, S.W. (1998a) 4Pi-confocal imaging in fixed biological specimens. *Biophys. J*. **75**, 1659–1668.

Schrader, M., Bahlmann, K. & Hell, S.W. (1997) Three-photon-excitation microscopy. Theory, experiments and applications. *Optik*, **104**, 116–124.

Schrader, M., van der Voort, H.T.M. & Hell, S.W. (1998b) Three-dimensional superresolution with a 4Pi-confocal microscope using image restoration. *J. Appl. Phys*. **84**, 4033–4042.

Schröck, E., du Manoir, S., Veldman, T., Schoell, B., Wienberg, J., Ferguson-Smith, M.A., Ning, Y., Ledbetter, D.H., Bar-Am., I., Soenksen, D., Garaini, Y. & Ried, T. (1996) Multicolor spectral karyotyping of human chromosomes. *Science*, **273**, 494–497.

Schütze, K., Clement-Sengewald, A. & Ashkin, A. (1994) Zona drilling and sperm insertion with combined laser microbeam and optical tweezers. *Fert. Steril*. **60** (4), 783–786.

Schwille, P., Haupts, U., Maiti, S. & Webb, W.W. (1999) Molecular dynamics in living cells observed by fluorescence correlation spectroscopy with one- and two-photon excitation. *Biophys. J*. **77**, 2251–2265.

So, P.T.C., König, K., Berland, K.M., Dong, C.Y., French, T., Buehler, C., Ragan, T. & Gratton, E. (1998) New time-resolved techniques in two-photon microscopy. *Cell. Mol. Biol*. **44**, 771–794.

So, P.T.C., Yu, W.M., Berland, K.M., Dong, C.Y. & Gratton, E. (1995) Time-resolved fluorescence microscopy using two-photon excitation. *Bioimaging*, **3**, 1–15.

Soeller, C. & Cannell, M.B. (1996) Construction of a two-photon microscope and optimisation of illumination pulse duration. *Eur. J. Physiol*. **432**, 555–561.

Speicher, M.R., Ballard, S.G. & Ward, D.C. (1996) Karyotyping human chromosomes by combinatorial multi-fluor FISH. *Nature Genet*, **12**, 368–375.

Squirrel, J.M., Wokosin, D.L., White, J.G. & Bavister, B.D. (1999) Long-term two-photon fluorescence imaging of mammalian

embryos without compromising viability. *Nature Biotechnol.* **17**, 763–762.

Stelzer, E.H.K., Hell, S., Lindek, S., Stricker, R., Pick, R., Storz, C., Ritter, G. & Salmon, N. (1994) Non-linear absorption extends confocal fluorescence microscopy into the ultra-violet regime and confines the illumination volume. *Opt. Commun.* **104**, 223–228.

Straub, M. & Hell, S.W. (1998) Fluorescence lifetime three-dimensional microscopy with picosecond precisionusing a multifocal multiphoton microscope. *Appl. Phys. Lett.* **73**, 1769–1771.

Straub, M. & Hell, S.W. (1998) Multifocal multiphoton microscopy: a fast and efficient tool for 3-D fluorescence imaging. *Bioimaging*, **6**, 177–185.

Summers, R.G., Piston, D.W., Harris, K.M., John, B. & Morrill, J.B. (1996) The orientation of first cleavage in the sea urchin embryo, *Lytechinus variegatus*, does not specify the axes of bilateral symmetry. *Develop. Biol.* **175**, 177–183.

Teuchner, K., Freyer, W., Leupold, D., Volkmer, A., Birch, D.J.S., Altmeyer, P., Stücker, M. & Hoffmann, K. (1999) Femtosecond two-photon excited fluorescence of melanin. *Photochem. Photobiol.* **70**, 146–151.

Tirlapur, U.K., Dahse, I., Reiss, B. & Oelmuller, R. (1999) Characterisation of the activity of a plastid targeted green fluorescent protein in *Arabidopsis*. *Eur. J. Cell Biol.* **78**, 233–240.

Tirlapur, U.K. & König, K. (1999) Near infrared femtosecond laser pulses as a novel non-invasive means for dye-permeation and 3D imaging of localised dye-coupling in the *Arabidopsis* root meristem. *Plant J.* **20**, 363–370.

Tyrell, R.M. & Keyse, S.M. (1990) The interaction of UVA radiation with cultured cells. *J. Photochem. Photobiol.* **4**, 349–361.

Veigel, C., Coluccio, L.M., Jontes, J.D., Sparrow, J.C., Milligan, R.A. & Molley, J.E. (1999) The motor protein myosin-I produces its working stroke in two steps. *Nature*, **398**, 530–533.

Wachter, E.A., Petersen, M.G. & Dees, H.C. (1999) Photodynamic therapy with ultrafast lasers. *SPIE-Proceed.* **3616**, 66–74.

Xu, C., Guild, J., Webb, W.W. & Denk, W. (1995) Determination of absolute two-photon excitation cross sections by *in situ* second-order autocorrelation. *Opt. Lett.* **20** (23), 2372–2374.

Xu, C. & Webb, W.W. (1996) Measurement of two-photon cross-sections. *J. Opt. Soc. Am. B.* **13** (3), 481–491.

Xu, C. & Webb, W.W. (1997) Multiphoton excitation of molecular fluorophores and non-linear laser microscopy. *Topics in Fluorescence Spectroscopy*, Vol. 5: *Non-Linear and Two-Photon Induced Fluorescence* (ed. by J. Lakowicz), pp. 471–540. Plenum Press, New York.

Yamashita, Y., Moriyasu, F., Ono, S., Kimura, T., Kajimura, K., Someda, H., Hamato, N., Nabeshima, M., Sakai, M. & Okuma, M. (1991) Photodynamic therapy using pheoporbide-a and Q-switched Nd: YAG laser on implanted human hepatocellular carcinoma. *Gast. Jap.* **26**, 623–627.